Title

Development and Application of FASA, a Model for Quantifying Fatty Acid Metabolism Using Stable Isotope Labeling

Journal

Cell Reports, 25(10)

ISSN

2639-1856

Authors

Argus, Joseph P
Wilks, Moses Q
Zhou, Quan D
et al.

Publication Date

2018-12-01

DOI

10.1016/j.celrep.2018.11.041

Peer reviewed

HHS Public Access

Author manuscript

Cell Rep. Author manuscript; available in PMC 2019 March 25.

Published in final edited form as:

Cell Rep. 2018 December 04; 25(10): 2919–2934.e8. doi:10.1016/j.celrep.2018.11.041.

Development and Application of FASA, a Model for Quantifying Fatty Acid Metabolism Using Stable Isotope Labeling

Joseph P. Argus[1], **Moses Q. Wilks**[2], **Quan D. Zhou**[1,3], **Wei Yuan Hsieh**[4], **Elvira Khialeeva**[5], **Xen Ping Hoi**[4], **Viet Bui**[6], **Shili Xu**[1], **Amy K. Yu**[1], **Eric S. Wang**[1], **Harvey R. Herschman**[1,5], **Kevin J. Williams**[4], and **Steven J. Bensinger**[1,4,7,*]

[1]Department of Molecular and Medical Pharmacology, David Geffen School of Medicine, University of California, Los Angeles, 615 Charles E. Young Drive East, Los Angeles, CA 90095, USA

[2]Gordon Center for Medical Imaging, Massachusetts General Hospital, Harvard Medical School, 149, 13th Street, Charlestown, MA 02129, USA

[3]Department of Surgical Oncology, The First Affiliated Hospital, School of Medicine, Zhejiang University, Hangzhou, Zhejiang 310003, P.R. China

[4]Department of Microbiology, Immunology, and Molecular Genetics, David Geffen School of Medicine, University of California, Los Angeles, 615 Charles E. Young Drive East, Los Angeles, CA 90095, USA

[5]Molecular Biology Institute, University of California, Los Angeles, 611 Charles E. Young Drive East, Los Angeles, CA 90095, USA

[6]Division of Rheumatology, David Geffen School of Medicine, University of California, Los Angeles, 1000 Veteran Avenue, Los Angeles, CA 90095, USA

[7]Lead Contact

SUMMARY

It is well understood that fatty acids can be synthesized, imported, and modified to meet requisite demands in cells. However, following the movement of fatty acids through the multiplicity of these metabolic steps has remained difficult. To better address this problem, we developed Fatty Acid Source Analysis (FASA), a model that defines the contribution of synthesis, import, and elongation pathways to fatty acid homeostasis in saturated, monounsaturated, and polyunsaturated

*Correspondence: sbensinger@mednet.ucla.edu.

AUTHOR CONTRIBUTIONS

J.P.A. conceptualized the project, designed and executed experiments, wrote script for the models, analyzed data, and constructed the manuscript. M.Q.W. designed experiments, wrote script for the models, and analyzed data. Q.D.Z. designed and executed experiments, wrote script for the models, and analyzed data. W.Y.H., E.K., X.P.H., V.B., S.X., A.K.Y., E.S.W., and K.J.W. designed and executed experiments and analyzed data. H.R.H. provided scientific advice. S.J.B. conceptualized the project, provided resources and supervision, and constructed the manuscript.

SUPPLEMENTAL INFORMATION

Supplemental Information includes twelve figures and five tables and can be found with this article online at https://doi.org/10.1016/j.celrep.2018.11.041.

DECLARATION OF INTERESTS

The authors declare no competing interests.

fatty acid pools. Application of FASA demonstrated that elongation can be a major contributor to cellular fatty acid content and showed that distinct pro-inflammatory stimuli (e.g., Toll-like receptors 2, 3, or 4) specifically reprogram homeostasis of fatty acids by differential utilization of synthetic and elongation pathways in macrophages. In sum, this modeling approach significantly advances our ability to interrogate cellular fatty acid metabolism and provides insight into how cells dynamically reshape their lipidomes in response to metabolic or inflammatory signals.

Graphical Abstract

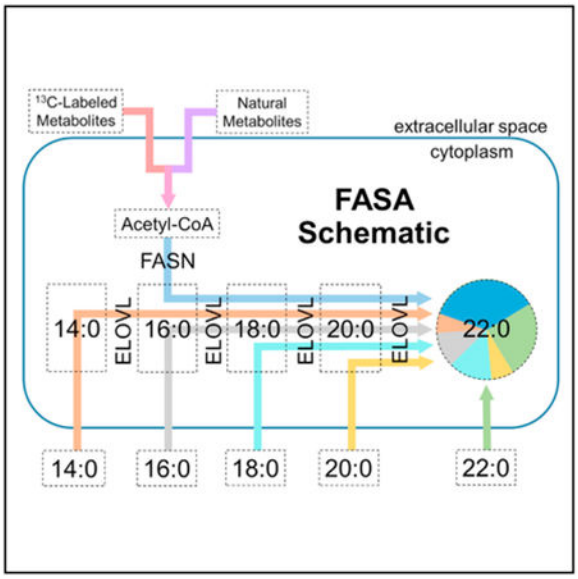

In Brief

Argus et al. developed Fatty Acid Source Analysis (FASA), a model that quantifies cellular fatty acid synthesis, elongation, and import. FASA is used to demonstrate that elongation can be a major contributor to cellular fatty acid content and that different stimuli reprogram macrophage fatty acid elongation pathways in distinct ways.

INTRODUCTION

Individual cells meet their fatty acids requirements through a combination of synthesis, import, and modification pathways (Vance and Vance, 2008). Long-chain fatty acids (LCFAs; 14 to 18 carbons) are synthesized through the enzymatic action of fatty acid synthase (FASN), producing primarily palmitic acid (16:0) and, to a lesser extent, 14:0 and 18:0 through the condensation of acetyl-coenzyme A (CoA) with malonyl-CoA (Vance and Vance, 2008; Wakil, 1989). These direct LCFA products of FASN can be further modified by both elongation and desaturation. The fatty acid desaturation pathways selectively oxidize fatty acids, introducing desaturations into the aliphatic tails. The fatty acid elongation enzymes lengthen a wide variety of fatty acids by 2 carbons per cycle through addition of malonyl-CoA (derived from acetyl-CoA) (Vance and Vance, 2008). In addition to synthesis, elongation, and desaturation, fatty acids can be imported directly from the extracellular space. These imported fatty acids can also enter cellular elongation or

desaturation pathways as required (Sassa and Kihara, 2014; Vance and Vance, 2008). In combination, these metabolic pathways allow cells to generate a wide variety of fatty acids commonly ranging from 14 to 24 carbons for use as free fatty acids and for incorporation into complex lipids. Consequently, the development of models that are capable of unraveling the complex nature of fatty acid homeostasis will be important for elucidating how cells achieve their cellular lipid composition under normal conditions and the extent to which these pathways are deranged in pathologic states.

The multiplicity of metabolic pathways contributing to fatty acid pools makes identifying the "source" of a fatty acid nearly impossible without the use of labeling strategies. Isotopomer spectral analysis (ISA) and mass isotopomer distribution analysis (MIDA) are independent modeling approaches that infer fatty acid metabolic parameters using mass spectrometry data from cells or tissues cultured with stable isotope-labeled metabolites such as glucose or glutamine (Hellerstein and Neese, 1992; Kelleher and Masterson, 1992). In classical ISA and MIDA models, there is an underlying assumption that fatty acids are either synthesized by FASN (often termed *de novo*-synthesized) or imported. This assumption results in modeling the empirical isotopologue distribution as two sub-distributions, a "light" distribution representing imported fatty acid and a "heavy" distribution representing synthesized fatty acid. From these distributions, one determines the relative contribution of the *de novo* synthesis and import pathways to fatty acid pools. However, because elongation of imported fatty acids is not fundamentally incorporated into these models, their utility is largely restricted to fatty acids for which the contribution of elongation to the pool is minimal (e.g., 14- and 16-carbon species). Subsequent iterations of these models include single elongation of imported fatty acid species, extending utility to 18-carbon fatty acids (Lee et al., 1994b; Lligona-Trulla et al., 1997; Oosterveer et al., 2009). More recently, a MATLAB-based algorithm (termed convISA) was developed to perform ISA with the option of single elongation (Tredwell and Keun, 2015), and it has already allowed greater access to this methodology (Gelman et al., 2018; Lau et al., 2017; Yao et al., 2016). However, it is likely that very-long-chain fatty acid (VLCFA; 20 to 24 carbons) pools include multiply elongated fatty acids. This complexity makes modeling the metabolism of these fatty acid species difficult and often inaccurate when using ISA or other similar models, limiting interrogation of how these fatty acid pools are regulated. This is a critical gap in current methodology because VLCFAs play essential roles in signaling and membrane structure in eukaryotic cells (Sassa and Kihara, 2014; Vance and Vance, 2008).

To address this barrier in understanding cellular fatty acid metabolism, we developed Fatty Acid Source Analysis (FASA), an approach that models both single and multiple elongations of imported fatty acids in addition to modeling *de novo* synthesis and direct import. Application of FASA significantly increases accuracy when defining the sources of fatty acids contributing to the very-long-chain saturated, monounsaturated, and polyunsaturated fatty acid pools found within the cellular lipidome. In addition, application of FASA at metabolic and isotopic steady state revealed previously unmeasured aspects of fatty acid metabolism in cells. Examination of a cancer cell line demonstrated that upward of 80% of 20- to 24-carbon saturated and monounsaturated fatty acid species can be products of the elongation machinery. Using FASA, we also provide evidence that the acetyl-CoA pools contributing to both fatty acid synthesis and elongation pathways can behave as a well-

mixed pool. Finally, application of FASA to primary macrophages revealed that Toll-like receptor (TLR) signaling has profound effects on synthetic and elongation pathway utilization. Taken together, these studies demonstrate the development and application of this approach to interrogate underappreciated aspects of cellular fatty acid metabolism.

RESULTS

Current Models Fail to Accurately Model Fatty Acids More Than 18 Carbons in Length

Cells maintain their fatty acid composition through a complex mixture of synthesis, import, and modification (e.g., desaturation and elongation) pathways (Vance and Vance, 2008). Stable isotope labeling and subsequent modeling of isotopologue distributions of fatty acids using ISA and MIDA allow accurate identification of the sources of LCFAs contributing to the cellular lipidome. Using these approaches, one can distinguish LCFAs that were synthesized by FASN from LCFAs that were directly imported or imported and then elongated once (Lee et al., 1994a; Lligona-Trulla et al., 1997; Oosterveer et al., 2009; Tredwell and Keun, 2015). However, many fatty acids in the cellular lipidome, such as VLCFAs, can be subject to multiple elongation events (Vance and Vance, 2008). Thus, we sought to ask whether application of ISA would accurately model VLCFAs.

To address this, human lung cancer-derived H1299 cells containing a stably incorporated doxycycline-inducible *shCON* (designated H1299 *shCON*) were cultured in medium containing 2% fetal bovine serum (FBS), 100% U-$^{13}C_6$ glucose, and 100% U-$^{13}C_5$ glutamine for 48 hr. After labeling, cellular lipids were derivatized, and isotopologue distributions for the resulting fatty acid methyl esters (FAMEs) were determined by gas chromatography-mass spectrometry (GC-MS). For this and all other experiments, the natural abundance of carbon, hydrogen, and oxygen isotopes was accounted for (see figure legends; STAR Methods). For each figure, isotopologue distribution data (before any correction for abundance of natural isotopes) are provided in Table S1. ISA was employed to determine the contribution of synthesis, import, and import with single elongation to the indicated cellular fatty acid pools. Note that, when performing ISA, we used convISA, a recent and publicly available MATLAB-based implementation of ISA (Tredwell and Keun, 2015). As expected, visual inspection revealed that ISA model fits were excellent for 14- to 18-carbon LCFA species (Figures 1A, S1A, and S1B). However, we observed that ISA model fits deteriorate as fatty acid carbon chains become longer (i.e., 20–24 carbons; Figures 1B, 1C, and S1D). For example, inspection of the best fit for the fatty acid 20:0 revealed a noticeable M+4 abundance ISA could not account for (Figure 1B, blue bracket on isotopologue distribution). Best fits for 22:0 and 24:0 revealed that ISA had difficulty finding the true FASN-synthesized (referred to hereafter as synthesized) distribution (Figures 1C and S1D, blue bracket on isotopologue distribution) and instead fit intermediate masses as the main components of the synthesized distribution (Figures 1C and S1D, red bracket). Similar results were seen with murine bone marrow-derived macrophages (BMDMs) and primary human fibroblasts (Figures S3A–S3C and S5A–S5C). Analysis of the sum of squared errors (SSEs) between the empirical isotopologue distribution and the ISA model fitting confirmed significant error in the modeled data for fatty acids longer than 18 carbons (Figure 1D). Similar SSE results were seen with murine BMDMs (Figure S3D). Taken together, these

data demonstrate that ISA provides accurate modeling of LCFAs containing up to 18 carbons but becomes less accurate as the fatty acid chain length increases.

Development of FASA, a Model that More Accurately Defines VLCFA Metabolism in Cells

ISA modeling assumes that fatty acids are fully synthesized, directly imported, or imported and elongated once. Parameter D of ISA modeling represents the fractional contribution of ^{13}C-labeled metabolites to the lipogenic acetyl-CoA pool. Correspondingly, 1-D represents the fractional contribution of natural metabolites to the lipogenic acetyl-CoA pool. Parameter $g(t)$ represents the percentage of a given fatty acid pool that has been synthesized at time t (Kelleher and Masterson, 1992; Kelleher and Nickol, 2015). Parameter $g4(t)$ represents the percentage of a given fatty acid pool that has been elongated once from an unlabeled shorter fatty acid. 1-$g(t)$-$g4(t)$ defines the unlabeled fraction of a given fatty acid pool. For simplicity, we designate $g(t)$, $g4(t)$, and 1-$g(t)$-$g4(t)$ as S (*de novo*-synthesized by FASN), IE_1 (imported-elongated once), and I (imported). Before steady state is achieved, the imported pool (I) is a mixture of newly imported and pre-existing fatty acids, whereas the IE_1 pool is a mixture of newly imported and pre-existing fatty acids that have been elongated once (Buescher et al., 2015).

Elongation of fatty acids relies on the condensation of carbons from the acetyl-CoA pool. We reasoned that the intermediate masses observed in the isotopologue distributions of VLCFAs (see Figures 1B and 1C for examples) resulted from multiple rounds of enzymatic condensation of ^{13}C-labeled carbons from the acetyl-CoA pool and that this accumulation of intermediate masses likely interferes with accurate model fitting using conventional approaches. To overcome this barrier in modeling, we created an approach, FASA, that allows fatty acids to be either synthesized (S), imported (I), or elongated (singly or multiply) from imported fatty acid species (designated IE_n, where n is the number of elongations after import) as short as 14:0 (Figure 2A). Incorporation of the imported-elongated parameters (IE_n) results in one additional distribution per two-carbon increase in length from 14:0.

FASA also allows direct modeling of the lipogenic acetyl-CoA pool. Multiple turns of the tricarboxylic acid (TCA) cycle can result in lipogenic acetyl-CoA that contains one carbon from a labeled metabolite and a second carbon from an unlabeled metabolite in a phenomenon we termed “label diffusion.” Label diffusion can cause an increased abundance of odd-numbered isotopologues and decreased even-numbered isotopologues compared with what would be expected without label diffusion, a phenomenon that has been reported previously (Collins et al., 2011) and that we have also observed in certain cases (e.g., Figure S6A). To ameliorate this issue, we designed FASA to allow the user to define whether to model the dilution of ^{13}C-labeled metabolites into the lipogenic acetyl-CoA pool (parameters D and 1-D) or to model the frequency of lipogenic acetyl-CoAs with 0, 1, and 2 ^{13}Cs using parameters D_0, D_1, and D_2. The same D from ISA (the fractional contribution of ^{13}C-labeled metabolites to the lipogenic acetyl-CoA pool) can still be calculated from D_0, D_1, and D_2 (STAR Methods), but this addition also allows the potential to account for and measure changes in label diffusion. For consistency, when applying FASA in this study, we modeled parameters D_0, D_1, and D_2. To determine the metabolic parameter values (i.e., D_0, D_1, D_2, S, I, IE_1, etc.) that result in the best fit for a given isotopologue distribution, we

developed a MATLAB-based script that uses a constrained gradient descent optimization to minimize the SSE between the empirical and modeled isotopologue distributions for each fatty acid in each sample. Monte Carlo replicates with random parameter starting points were performed to ensure that the global minimum of the SSE function was found (STAR Methods).

Visual inspection of 14- to 18-carbon fatty acid isotopologue distributions using FASA revealed equivalent or slightly improved fits compared with ISA (Figures 2B, S1A, S1B, S2A–S2C, and S4A–S4C). Accordingly, model-derived parameters such as S, IE_1, I, and D were nearly identical between ISA and FASA (Figures 2C, 2G, S1A, S1B, S2A–S2C, S3E, S4A–S4C, and S5E) for these LCFAs. Importantly, analysis of isotopologue distributions for VLCFAs with FASA resulted in significantly better visual fits compared with ISA, ameliorating the issues with modeling the intermediate masses (Figures 2D, S1C, S1D, S3A–S3C, and S5A–S5C). Model-derived parameters (e.g., S, I, and IE_1) were significantly adjusted, and contributions of multiple elongations to the fatty acid pool were now quantifiable (Figures 2E, 2G, S1C, S1D, S3A–S3C, S3E, S5A–S5C, and S5E). For example, in 24:0, shorter imported fatty acids that had been multiply elongated made up a significant portion (≈35%) of the pool in H1299 *shCON* cells (Figure 2E). Similar results were seen with murine BMDMs (≈40%; Figure S3C) and primary human fibroblasts (≈35%; Figure S5C). Consistent with better visual fits, the SSEs were significantly lower for fatty acids containing 20 or more carbons when using FASA (Figures 2F, S3D, and S5D). Results from log-likelihood ratio tests also indicated that FASA's superior fits for these longer fatty acids were not due to increased parameter number alone ($p \leq 0.05$; STAR Methods; Table S2). Together, these results demonstrate the value of including parameters for multiple elongations when modeling fatty acids longer than 18 carbons.

When applying FASA to H1299 *shCON* cells, we observed that the model-derived values for D were consistent across all LCFA and VLCFA species measured (Figure 2G). Similar results for D were seen in studies of macrophages and primary human fibroblasts (Figures S3E and S5E). This observation for D is consistent with concept that the acetyl-CoA and malonyl-CoA pools available to both FASN and elongation machinery (i.e., ELOVL1-7) can be equivalently labeled from the isotope-labeled metabolite precursors (in this case, U-$^{13}C_6$-glucose and U-$^{13}C_5$-glutamine). Thus, we conclude that the acetyl-CoA pool contributing to both the fatty acid synthetic and elongation pathways (the lipogenic acetyl-CoA pool) can behave as a single well-mixed pool rather than distinct pools with different contributions of isotope labels. Although spatially separated acetyl-CoA pools exist within the cell (e.g., cytosolic [Vance and Vance, 2008], endoplasmic reticulum [ER; Jonas et al., 2010], mitochondrial [Vance and Vance, 2008], peroxisomal [Wong et al., 2004], and nuclear [Bulusu et al., 2017]), these different pools are either isotopically equivalent to the lipogenic acetyl-CoA pool or do not significantly contribute to fatty acid metabolic processes under the conditions tested here.

To provide evidence that FASA can detect specific changes in elongation, we applied FASA to isotopologue distributions for LCFAs and VLCFAs from H1299 cells where *ELOVL1* expression was transiently silenced using small interfering RNAs (siRNAs). *siControl*- and *siELOVL1*-treated cells were cultured in medium containing 2% FBS and 100% U-$^{13}C_6$-

glucose. Cells were collected for mRNA and fatty acid analysis after 24 hr and 48 hr of labeling, respectively. ELOVL1 preferentially elongates VLCFA and should have little effect on LCFA elongation, which is largely regulated by the elongase ELOVL6 (Vance and Vance, 2008). Analysis of mRNA confirmed a significant decrease in *ELOVL1* gene expression (≈10% of control; Figure S6B). A modest but statistically significant increase in *ELOVL6* was also seen, likely as a compensatory effect (Figure S6B). Importantly, analysis of fatty acid isotopologue distributions using FASA revealed that silencing of *ELOVL1* had a significant effect on the contribution of elongation to the cellular 22:0 and 24:0 pool (Figure S6C). In contrast, the contribution of elongation to the 16:0, 18:0, and 20:0 pools remained unchanged (Figure S6C). These results provide proof of concept that FASA can be applied to isotope labeling studies to detect specific changes in the utilization of cellular elongation pathways.

Inclusion of Parameter Constraints in FASA to Accommodate Polyunsaturated Fatty Acid Elongation

In mammals, essential polyunsaturated fatty acids (PUFAs) are not synthesized *de novo* (Le et al., 2009), and mammalian cells rely on import of these fatty acids from the diet (e.g., 18:2n-6, 18:3n-3). Upon import, these fatty acids are elongated and/or desaturated to create a wide variety of requisite PUFAs (Vance and Vance, 2008). Because FASA allows for import and multiple elongation of fatty acids, we thought it possible that FASA could be applied to model elongation of PUFAs. Furthermore, we designed FASA to allow users to easily constrain model parameters to any specific value *a priori* as part of the input data Excel file. For example, when analyzing n-6 or n-3 PUFAs, one can set the S parameter (representing synthesized fatty acids) to zero because mammalian cells cannot synthesize these fatty acids *de novo*. One can also set the D_0, D_1, and D_2 parameters to values determined from other more abundant fatty acids (for instance, using D_0, D_1, and D_2 defined from 16:0 to model other fatty acids in the same sample). Although defining these parameters *a priori* adds additional assumptions, it effectively constrains the parameter space when only a few isotopologues are measurable, a common occurrence with PUFAs.

With these concepts in mind, we asked whether FASA would be capable of modeling n-6 PUFA metabolism in cells. Linoleic acid (18:2n-6) is an essential PUFA that serves as the substrate for synthesis of other n-6 PUFAs via the actions of elongases and desaturases (Figure 3A; Vance and Vance, 2008). Therefore, we set the parameters for synthesis (S) and import-elongation from 14 and 16 carbons (IE_2–IE_3 for 20-carbon PUFA and IE_3–IE_4 for 22-carbon PUFA) to zero. We also fixed the D_0, D_1, and D_2 parameter values to reflect the parameter values obtained from 16:0. Visual inspection of FASA-generated isotopologue distributions for 22:4n-6 from H1299 *shCON* cells, BMDMs, and primary human fibroblasts revealed good fits compared with empirical data (Figures 3B, S7A, and S7C). For the three cell types tested, we found that a sizeable portion of the 22:4n-6 pool was generated via elongation (IE_1 ≈25%-40% and IE_2 ≈0%–10%; Figures 3C, S7A, and S7C).

Interestingly, we observed evidence of double elongation into the 20:3n-6 pool for all three cell types tested. Inspection of the empirical 20:3n-6 isotopologue distributions revealed the presence of an M+4 isotopologue (Figures 3D, S7B, and S7D), indicating a non-zero

contribution of double elongation to the 20:3n-6 pool despite an expectation of only single elongation. Therefore, we included an additional import-elongation distribution for this PUFA to accommodate elongation from 16 carbons when applying FASA (Figures 3A, 3D, S7B, and S7D). For the three cell types tested (H1299 *shCON* cells, murine BMDMs, and primary human fibroblasts), a notable portion of the 20:3n-6 pool was generated through elongation (IE_1 ≈5%–35% and IE_2 ≈5%–15%; Figures 3E, S7B, and S7D). The origin of 16:2n-6 in these cells remains to be determined, and it is possible that plant-derived 16:2n-6 could be present in our culture media. Alternatively, it may be that some percentage of 18:2n-6 is shortened into a 16:2n-6 species before subsequent elongation. Additionally, it is not clear which enzyme(s) would be involved in the elongation of 16:2n-6. One or more ELOVLs are likely candidates; however, for simplicity in our elongation diagrams (Figures 2A and 3A), we only list specific ELOVLs known to have strong activity for a given substrate (Sassa and Kihara, 2014). Taken together, these studies provide proof of concept that FASA can model PUFAs and can measure underappreciated aspects of fatty acid metabolism within a cell.

Determining Minimum Parameter Levels for Accurate Modeling

One limitation of any stable isotope modeling approach for lipid metabolism occurs when isotope labeling of the lipid of interest is low. As the amount of stable isotope label in the acetyl-CoA pool decreases, the synthesis (S) and import-elongated (IE_n) distributions will approach the imported (I) distribution, making model fitting progressively more difficult. Therefore, we sought to determine the minimal amount of labeling of the acetyl-CoA pool (parameter D when ^{13}C-enrichment in the labeled metabolites (e) is at or near 100%) required for FASA to effectively fit the distributions in LCFA and VLCFA isotopologue distributions.

To this end, H1299 *shCON* cells were cultured for 48 hr in medium containing 2% FBS and increasing percentages of U-$^{13}C_6$ glucose and U-$^{13}C_5$ glutamine. After labeling, the cells were collected, and fatty acid isotopologue distributions were determined. Modeling of isotopologue distributions with FASA revealed that model parameter D behaved in a linear fashion with respect to the percentage of ^{13}C-labeled metabolites in the medium down to D ≈30% for 14:0–24:0. Shorter fatty acids remained linear down to D ≈ 10%, the lowest labeling level tested (Figure S8A). In most cases, the S and I model parameters (FASN-synthesized and imported, respectively) were consistent as long as D was in the linear range described above (Figure S8B). However, for elongation parameters (IE_n), we observed that a variable level of labeling in the lipogenic acetyl-CoA pool was required for consistent determination. For example, when examining the elongation parameters of 22:0, we observed that the IE_1 and IE_4 parameters were consistent down to a D of ≈40% (Figure S8B). In contrast, IE_2 and IE_3 required higher levels of labeling to achieve consistent values (D ≈50%) (Figure S8B). From these studies, we conservatively conclude that FASA will most consistently model 14- to 24-carbon fatty acids when the lipogenic acetyl-CoA pool is labeled to at least 50% (Figures S8C and S8D).

We further explored this issue using *in silico*-based sensitivity analyses to determine the robustness of FASA to variations in input data and noise. To test D, a realistic parameter set

for fatty acid sources was chosen for each fatty acid length (based on empirical data), and D was varied from 5% to 80% (STAR Methods). Theoretical isotopologue distributions were generated from the parameter sets, and multiple realizations of Gaussian noise were added to each theoretical isotopologue distribution. Each of these realizations was analyzed by FASA. For both expected and high noise levels, nearly all parameters were well-defined (≤10% bias) in our biologically relevant test cases when D was greater than or equal to 50%, agreeing with our *in vitro* experiment above (Figure S9 and data not shown). We observed somewhat higher biases (10%–45%) for a few parameters. However, these larger biases occurred in lower abundance imported-elongated parameters that are generally combined with larger, more stable parameters in subsequent analyses (see below). We also found that increasing D above 50% lowered the bias of these outliers to below 10%.

Similar *in silico* tests were run to determine accuracy of fits when varying S and IE_{max} (the imported-elongated distribution with the most elongations) values. When testing these parameters, empirically derived intermediate values for D_0, D_1, and D_2 were held constant, whereas S or IE_{max} were varied from 1%–90% or 0.1%–8%, respectively (STAR Methods). Under expected noise conditions, all parameters were well-defined (≤10% bias) when $S \geq 5\%$, and under high noise conditions, the large majority of parameters had low to modest bias (≤25%) when $S \geq 5\%$ (Figure S10 and data not shown). When $IE_{max} \geq 1\%$, all parameters were well-defined (≤10% bias) under expected noise conditions, and under high noise conditions, there were only a few outliers (10%–30% bias; Figure S11 and data not shown). In sum, we provide *in vitro* and *in silico* evidence that FASA parameters can be determined accurately for realistic noise levels and parameter values.

Application of FASA Reveals a Significant Contribution of Elongation Pathways to Fatty Acid Homeostasis

Translation of labeling data and modeling parameters into metabolic information is complex and depends on both the system and the labeling conditions (Buescher et al., 2015). Interpretation of FASA parameters as well as parameters from many other stable isotope labeling models is simplified when measurements are made at isotopic and metabolic steady state (iSS and mSS, respectively) (Buescher et al., 2015). A metabolite pool reaches iSS when its isotopologue distribution remains constant over time, whereas a metabolite pool reaches mSS when its size and fluxes remain constant over time (Buescher et al., 2015). Key advantages for applying FASA at iSS and mSS are that pre-existing, and therefore unlabeled, pools of fatty acids have been diluted out, and fluxes are constant. This allows unambiguous identification of unlabeled fatty acids as imported and allows one to determine the relative contribution of different sources to a given fatty acid pool (e.g., FASN-synthesized versus imported) (Buescher et al., 2015). Although these steady-state conditions are hard to ensure in any system, culturing cells for an extended period of time in the presence of stable isotope metabolites can approximate iSS and mSS (Buescher et al., 2015).

To study cells at iSS and mSS, H1299 cells were cultured in medium containing 5% FBS and 100% U-$^{13}C_6$-glucose for 5 days (approximately 5 cell divisions). The culture medium was refreshed every 12 hr, and cells were maintained in a subconfluent state. After collection, fatty acid isotopologue distributions were determined and modeled using FASA.

In line with our previous data (Figure 2G), *D* was remarkably consistent across all measured saturated fatty acids (SFAs) and monounsaturated fatty acids (MUFAs; Figure 4A). Analysis of individual SFA and MUFA species from 16 to 24 carbons in length revealed that individual fatty acid pools are indeed an admixture of imported, synthesized, and imported-elongated fatty acids (Figure 4B and data not shown). For example, modeling of the 20:0 fatty acid pool indicates that ≈45% of the pool is derived from fatty acids that were synthesized by FASN and subsequently elongated, ≈15% is directly imported, and ≈40% of the 20:0 fatty acids were imported as shorter species (14:0, 16:0, or 18:0) and then subject to elongation (IE_1 ≈20% [18:0 to 20:0], IE_2 ≈ 15% [16:0 to 20:0], and IE_3 ≈5% [14:0 to 20:0]). These results underscore the importance of using a model that includes the possibility of multiple elongations to imported fatty acids, particularly when analyzing VLCFAs.

In classical ISA, *S* and *I* at mSS and iSS represent the contribution of *de novo* synthesis and import to a particular fatty acid pool (Kelleher and Nickol, 2015; Metallo et al., 2011). In addition, the ratio of *S* to *I* represents the ratio of the synthetic and import fluxes when two additional assumptions are made: that *de novo* synthesis and import are the only contributions to the pool and that there is no preferential loss from the pool (Buescher et al., 2015). These concepts can be generalized in FASA; the contribution of import and elongation to a particular fatty acid pool with 18 or more carbons can be determined by comparing *I* with the sum of the other source parameters (Figure 4C). Relative fluxes of import and elongation can also be determined when the same additional assumptions are made. Note that, for fatty acid pools that are direct products of desaturation instead of elongation (e.g., 18:1n-9), elongation contribution can still be determined, but import will include both direct import and import followed by desaturation. Additionally, although the final product of FASN is primarily 16:0, it has been reported to produce 14:0 and 18:0 at lower frequency (Vance and Vance, 2008; Wakil, 1989). For simplicity, we assume that, with the exception of the 14:0 pool, all FASN products are 16:0 (STAR Methods).

Summation of the fatty acids subject to synthesis and elongation in the SFA and MUFA pools revealed that the elongation pathways contributed roughly 50%–75% of the 18-carbon species in the cell and 80%–95% for 20- to 24-carbon species (Figure 4D). Examination of select n-6 PUFAs revealed higher variation in elongation contribution, with approximately 15% of 20:3n-6 and 70% of 22:4n-6 having been elongated once or twice. These data demonstrate that elongation pathways can be an important metabolic conduit to meet a cell's fatty acid requirements.

Application of FASA to Pre-iSS and/or mSS Fatty Acid Pools

Although FASA can provide a significant amount of information about fatty acid origin and relative flux at iSS and mSS, it is difficult to achieve and/or maintain iSS and mSS for the required labeling period (often multiple days) in many model systems (Buescher et al., 2015; Metallo et al., 2011). Thus, we sought to determine what biological information can be ascertained from application of FASA when cells have not yet achieved iSS and/or mSS in fatty acid pools. To this end, H1299 *shCON* cells were treated with doxycycline for 96 hr; in the final 48 hr of doxycycline treatment, they were also labeled in medium containing 5%

FBS, 100% U-$^{13}C_6$-glucose, and 100% U-$^{13}C_5$-glutamine. H1299 *shCON* cells divide approximately twice over this labeling period; this time period is not sufficient to achieve iSS for the fatty acid pools of the cells (Metallo et al., 2011). After 48 hr of labeling, cells were counted on-plate, collected, and analyzed for fatty acid content. Note that, when applying ISA, FASA, or other similar models, we make the assumption that the lipogenic acetyl-CoA pool reaches iSS quickly compared with the total labeling time. Multiple relevant central carbon metabolites (including citrate) have been shown to approach isotopic steady state at or before 2 hr of labeling (Yoo et al., 2008), supporting the validity of this assumption for a 48-hr labeling period (STAR Methods).

Before iSS and/or mSS in the fatty acid pools is achieved, it is difficult to use FASA or other isotope labeling analyses to determine the contribution of import to a given fatty acid pool because the unlabeled fatty acid population of the cell is an unknown mixture of newly imported and pre-existing unlabeled fatty acids. However, application of FASA before iSS and/or mSS is achieved in fatty acid pools still allows one to quantify the accumulation of both *de novo*-synthesized (from FASN activity) and elongated fatty acids during the labeling period. For example, if pool size and cell numbers are known, then one can calculate the accumulation of elongated fatty acid in any measured fatty acid pool over the labeling period (STAR Methods). The results for this type of analysis for 20:3n-6 and 22:4n-6 are shown in Figure 5A.

If data exist for a large number of fatty acids in a single pathway, then one can go a step further and calculate the contribution of each pathway step to accumulated fatty acids. For example, FASA parameters determined before fatty acid pools have reached iSS and/or mSS can be used to determine the accumulation of SFA and MUFAs in the cellular lipidome that were directly elongated from 18 to 20 carbons. This includes elongation products that remained in the 20-carbon fatty acid pools and those that were subject to subsequent elongations and/or desaturation events. In this process, we first determine all SFAs and MUFAs that would have been subject to elongation from 18 to 20 carbons (Figure 5B). Note that SFA and MUFA of the same length are combined in this analysis because the relevant elongases acting on these fatty acids are similar (Sassa and Kihara, 2014; Vance and Vance, 2008). Multiplying these values by the final measured amount of each fatty acid pool divided by the average cell number on the plate during the entire isotope labeling period results in the contributions of each fatty acid to the total accumulation of 18 to 20 SFA and MUFA elongation products over the labeling period (Figure 5C). Summing these individual contributions provides the total accumulation of 18 to 20 SFA and MUFA elongation products (in nmol per 1e6 cells) during the labeling period (Figure 5D). This process can be repeated similarly for other elongation steps and for *de novo* synthesis to define the contribution of the elongation and synthetic machinery to fatty acid accumulation in the cell over the labeling time (Figures 5E and 5F; STAR Methods). Note that, for simplicity, we assume that, with the exception of the 14:0 pool, all FASN products are 16:0 (STAR Methods).

In proof-of-concept studies, we applied this approach to H1299 cells that have the sterol regulatory element binding protein (SREBP) transcriptional axis acutely disrupted using a doxy-cycline-inducible shRNA targeting the SREBP chaperone SCAP (Abel et al., 2013).

SREBPs are master transcriptional regulators of lipid homeostasis and are reliant on SCAP for their proper function (Horton et al., 2002; Matsuda et al., 2001). Cells were treated with doxycycline for 96 hr; in the final 48 hr of doxycycline treatment, they were also labeled in medium containing 5% FBS, 100% U-$^{13}C_6$-glucose, and 100% U-$^{13}C_5$-glutamine. After 48 hr of labeling, cells were collected for gene expression analysis or counted on-plate and collected for fatty acid analysis. The knockdown efficiency for *SCAP* was approximately 90% of control cells, and accordingly, the expression of SREBP target genes involved in fatty acid metabolism was also significantly decreased (Figure 6A) (Horton et al., 2002). Application of FASA, followed by the analytical approach described in Figures 5B–5D, demonstrated that loss of SREBP activity significantly decreased the accumulation of SFA and MUFAs that were synthesized by FASN and/or acted on by the elongation machinery (Figures 6B and 6C). A less significant effect on PUFA elongation was observed (Figures 6A and 6D). These data provide proof of concept that application of FASA before fatty acid pools have reached iSS and/or mSS can reveal an integrated picture of the accumulation of synthesized and elongated fatty acids in response to perturbations.

Macrophages Specifically Reprogram Elongation in Response to Inflammatory Stimuli

Macrophages rapidly reprogram their lipid metabolism in response to inflammatory signals. These changes in metabolism are critical for proper differentiation and function (O'Neill and Pearce, 2016; York et al., 2015; Zhang et al., 2017). To date, little is known about how TLR signals influence the flow of fatty acids through elongation pathways. To investigate this question, BMDMs were stimulated with a panel of TLR agonists (Pam3CSK4 [TLR2], poly(I:C) [TLR3], or lipopolysaccharide (LPS) [TLR4]) for 48 h in medium containing 5% FBS, 100% U-$^{13}C_6$-glucose, and 100% U-$^{13}C_5$-glutamine. Analysis of fatty acid isotopologue distributions was performed using FASA. Confidence intervals for FASA parameters from macrophage experiments are provided in Table S3. Analysis of the FASA results revealed that TLR2 activation significantly increased the accumulation of SFA and MUFA that were generated through FASN and/or elongation machinery (Figures 7A and 7B). In contrast, TLR3 stimulation resulted in the opposite metabolic program, with a profound decrease in the accumulation of SFA and MUFA generated through FASN and/or elongation pathways (Figures 7A and 7B). Interestingly, TLR4 stimulation produced more modest changes in accumulation through FASN and/or elongation pathways, resulting in an intermediate phenotype (Figures 7A and 7B).

Analysis of n-6 PUFAs revealed different metabolic reprogramming in response to these pro-inflammatory stimuli compared with SFA and MUFA (Figure 7C). TLR3 stimulation resulted in significant accumulation of elongated 22:4n-6, whereas TLR2 and TLR4 stimulation resulted in minimal changes. All three TLR ligands resulted in a modest decrease in accumulation of elongated 20:3n-6. Of note, we found that gene expression studies alone would not be able to predict the complex accumulation pattern we observed in the reprogramming of fatty acid elongation machinery. For example, we found that TLR2 activation resulted in similar or decreased expression levels of *Elovl6* and *Elovl3* (Figure 7D), whereas FASA demonstrated significant accumulation of the products of these enzymes. In other cases, the gene expression and modeling data are concordant, such as upregulation of *Elovl2* in response to TLR3 activation (Figure 7D) and the accumulation of

Elovl2 product 22:4 (Figure 7C). This provides evidence that FASA can reveal an integrated picture of different contributions to cellular fatty acid accumulation that can offer significantly more information than gene expression studies alone. We also asked whether FASA could model reprogramming of elongation during viral infections (Koyuncu et al., 2013). BMDMs were challenged with the γ-herpesvirus MHV-68 (MOI = 1) in medium containing 5% FBS, 100% U-$^{13}C_6$-glucose, and 100% U-$^{13}C_5$-glutamine for 48 hr before lipids were collected and analyzed as above. We observed a pattern of synthesis and elongation similar to that of TLR3-stimulated BMDMs (Figures 7E and 7F and S12A). Likewise, gene expression studies also indicated a significant upregulation of *Elovl2* in response to infection (Figure S12B), suggesting that reprogramming the elongation machinery is a physiologic response by the host to viral infection of cells. These data demonstrate that pro-inflammatory stimuli can reprogram the accumulation of fatty acids through synthetic and elongation pathways and that there is a high degree of specificity in these changes based on the type of inflammatory signal.

DISCUSSION

Understanding how lipids move through metabolic pathways under normal and disease states is of significant importance. Here we developed a model, FASA, that provides the ability to interrogate the contribution of synthesis, elongation, and import of fatty acids ranging from 14–24 carbons in length and 0–4 double bonds, covering the majority of fatty acids found in animal cells. FASA improves previous models such as ISA (or convISA) and MIDA by including several additional features relevant to modeling cellular fatty acid metabolism. First, we incorporate additional parameters not found in earlier models that allow single and multiple elongation of imported 14- to 22-carbon fatty acids. Second, we allow users to directly model the lipogenic acetyl-CoA pool. Third, we allow users to set multiple parameters *a priori*, facilitating the modeling of fatty acids (e.g., PUFA) and conditions (e.g., TLR3 stimulation) with little or no *de novo* synthesis. Finally, although FASA is a MATLAB algorithm, we have structured it so that minimal MATLAB experience is necessary to use it. The associated readme file contains instructions for use and descriptions of user handles. In addition, data inputs and outputs are in Excel format. The straightforward implementation of FASA will allow scientists with a wide range of computational backgrounds to utilize FASA to interrogate cellular fatty acid homeostasis. We anticipate that this model will lead to a better understanding of fatty acid metabolism in normal and disease states.

One of the largest challenges in stable isotope labeling is the appropriate interpretation of often complicated isotopologue distributions (Buescher et al., 2015). For FASA, examining cells at mSS and iSS will result in the simplest analysis. In this case, the key parameters for elongated fatty acids (18–24 carbons) are I and $1\text{-}I$ (Figure 4), which represent the contribution of import and elongation to a particular fatty acid pool, respectively. In many systems, although the lipogenic acetyl-CoA pool reaches iSS rapidly (Yoo et al., 2008), achieving mSS and iSS in fatty acid pools is not practically attainable. Information about the contribution of fatty acid import may be difficult to obtain under these conditions because of the confounding factor of cells containing pre-existing unlabeled fatty acid pools. Nevertheless, the accumulation of newly synthesized and imported-elongated fatty acids can

still be measured. These changes in accumulation provide useful biological information, but one must exercise caution when using changes in accumulation as a marker for changes in flux. In our studies, one cannot assess all of the modifications to fatty acids that may be occurring (e.g., β-oxidation) or the flow into unmeasured pools (e.g., SFA and MUFA, >24 carbons). As a result of these confounding factors, it is possible, and indeed likely, that the accumulation described here will be an underestimation of the absolute flux in a given cellular system. Despite these concerns, FASA provides important insights into the lipid metabolic state of the cell, and we envision that future work focused on building kinetic models to define absolute fluxes of these enzymatic pathways will likely require information provided by FASA or another similar approach.

The above *in silico* tests demonstrate the importance of treating high-noise isotopologue data and/or low parameter values with some care (Figures S9–S11). Note that, for many parameters modeled in the *in silico* tests, high noise resulted in high relative SDs (RSDs) (particularly for parameters with small values), even when the average percent error (bias) was reasonable. Furthermore, in fatty acids where there is very little labeling (e.g., 18:2n-6 and 20:4n-6 under the conditions tested here), small irregularities in the isotopologue distribution data (e.g., contaminants, ionization artifacts, error because of low signal) can potentially affect the modeling results. However, steps can be taken to ameliorate these issues. Cell culture conditions can potentially be modified to influence parameter values. If noise is relatively high, data collection protocols can be optimized to reduce error, and additional biological and/or technical replicates can be used to approach the true mean. When $S < 5\%$, increasing the number of Monte Carlo replicates can help to ensure that the correct synthetic distribution (producing the global minimum SSE) is found.

Finally, one assumption common to ISA, MIDA, and FASA is that the acetyl-CoA pool contributing to lipogenesis has a uniform labeling pattern (Hellerstein and Neese, 1992; Kelleher and Masterson, 1992). FASN is the major source of 14- to 16-carbon SFAs, and the elongases (ELOVL1-ELOVL7) are the major source of 18- to 24-carbon fatty acids (Vance and Vance, 2008). Given that FASN is a cytosolic enzyme and that ELOVLs are embedded in the ER facing the cytosol, it is not unreasonable to assume that the cytosolic acetyl-CoA pool is the major lipogenic acetyl-CoA pool in the cell (Vance and Vance, 2008). Although other groups have identified conditions under which the mitochondrial (Wong et al., 2004), nuclear (Bulusu et al., 2017), or peroxisomal (Wong et al., 2004) acetyl-CoA pools can differ in labeling pattern from that of the cytosolic acetyl-CoA pool, the contribution of those organelles to *de novo* synthesis is often relatively small (Vance and Vance, 2008). Furthermore, the data presented here are consistent with the hypothesis that the lipogenic acetyl-CoA can behave as a single well-mixed pool. The D values calculated independently for 14-24-carbon SFAs and MUFAs are very similar, in agreement with the assumption (Figures 2G, 4A, S3E, and S5E). However, it is possible that this assumption would not hold true with all cell types or culture conditions. Consequently, it will be important to validate that analyzed fatty acids for a given sample yield similar D values when different conditions or experimental systems are used. We also show that successful application for VLCFAs requires a fairly significant level of labeling in the acetyl-CoA pool (≥50%) to obtain good fits for the data. Alternatively, it may be possible to lower the labeling requirements for the

acetyl-CoA pool by using modeling to improve the accuracy of isotopologue peak integration (Krämer et al., 2018; Stein, 1999).

In conclusion, here we provide a model, FASA, that allows indepth characterization of fatty acid synthesis, elongation, and import in cells. Using FASA, we have demonstrated that fatty acid elongation pathways significantly contribute to LCFA and VLCFA homeostasis in cells. We also show that these pathways are dynamically and differentially regulated by distinct inflammatory signals, suggesting an importance in regulating these pathways during responses to different classes of pathogens. As a result, we anticipate that application of FASA will be useful to a wide variety of fields endeavoring to elucidate how fatty acid homeostasis affects cellular fate and function.

STAR★METHODS

CONTACT FOR REAGENT AND RESOURCE SHARING

Further information and requests for resources and reagents should be directed to and will be fulfilled by the Lead Contact, Steven J. Bensinger (sbensinger@mednet.ucla.edu).

EXPERIMENTAL MODEL AND SUBJECT DETAILS

Mice—6- to 8-week-old male C57BL/6J mice were purchased from Jackson Labs. All animal protocols were approved by the UCLA Animal Research Committee.

Cell Lines and Primary Cells—All cell lines and primary cells were maintained at 37°C in a humidified incubator containing 5% CO_2. All fetal bovine serum (FBS; Omega Biosciences, Atlanta Biosciences, VWR, HyClone) was heat-inactivated for 20 minutes at 55°C before use in media.

Parental H1299 Cells: H1299 (human male non-small cell lung cancer-derived; also referred to as NCI-H1299) cells were purchased from ATCC. Cells were passaged in DMEM (Thermo Fisher) supplemented with 10% FBS, 100 U/mL penicillin (Thermo Fisher), and 100 mg/mL streptomycin (Thermo Fisher) or RPMI 1640 (Thermo Fisher) supplemented with 10% FBS, 100 U/mL penicillin, 100 μg/mL streptomycin, and 10 mM HEPES (Thermo Fisher). Cells were dissociated using trypsin-EDTA (Thermo Fisher).

293FT Cells: 293FT cells were provided by Dr. Harvey Herschman (UCLA). Cells were maintained in DMEM supplemented with 10% FBS, 100 U/mL penicillin, 100 μg/mL streptomycin, 1 mM sodium pyruvate (Thermo Fisher), 1% MEM non-essential amino acids (Thermo Fisher), and 6 mM glutamine (Thermo Fisher). Cells were dissociated using trypsin-EDTA.

Stable, Inducible shRNA H1299 Cells Lines: Short hairpin RNAs (shRNA) were synthesized by Integrated DNA Technologies. Oligonucleotides were annealed and ligated into the pENTR/H1/TO vector (Thermo Fisher) following the BLOCK-iT Inducible H1 RNAi Entry Vector Kit manual. Resulting shRNA constructs were recombined into pLentipuro/BLOCK-iT-DEST (Abel et al., 2013) using Gateway LR Clonase II (Thermo Fisher) according to manufacturer instructions. The doxycycline induction of knockdown is

controlled by the Tet repressor (TetR) protein expressed from the pLenti0.3/EF/GW/IVS-Kozak-TetR-P2A-Bsd vector (Abel et al., 2013).

Recombinant lentiviruses were packaged in 293FT cells according to manufacturer instructions by co-transfecting cells with lentivirus plasmid and packaging plasmids pLP1, pLP2, and pLP/VSV-G (Thermo Fisher) using FuGENE 6 (Promega) as a transfection reagent. Viral supernatants were collected 72 hours after transfection. Parental H1299 cells were first transduced with viral supernatant (pLenti0.3/EF/GW/IVS-Kozak-TetR-P2A-Bsd) for 72 hours, followed by selection with blasticidin (40 μg/mL; Invivogen). The resulting cells were then transduced with viral supernatant (pLentipuro/BLOCK-iT-DEST) for 72 hours, followed by selection with blasticidin (40 μg/mL) and puromycin (4 μg/mL, Gemini).

The resulting H1299 *shCON* and H1299 *shSCAP* cell lines were passaged in DMEM supplemented with 10% FBS, 100 U/mL penicillin, 100 μg/mL streptomycin, 10 mM HEPES, and 2 μg/mL puromycin. Cells were dissociated using trypsin-EDTA.

Primary Human Fibroblasts: Primary human fibroblasts (male) were obtained from the Coriell Institute. The fibroblasts were passaged in DMEM supplemented with 10% FBS, 100 U/mL penicillin, and 100 μg/mL streptomycin. Cells were dissociated using trypsin-EDTA.

Murine Bone Marrow-Derived Macrophages: Murine bone marrow-derived macrophages (BMDMs) were generated as previously described (Divakaruni et al., 2018; York et al., 2015). Briefly, bone marrow cells were isolated from femurs of 6- to 8-week-old male C57BL/6J mice. Cells were treated with RBC lysis buffer (Sigma-Aldrich) for 5 minutes to remove red blood cells, centrifuged at 386xg for 5 minutes, and resuspended in BMDM culture medium. BMDM culture medium consisted of DMEM supplemented with 10% FBS, 100 U/mL penicillin, 100 mg/mL streptomycin, 500 μM sodium pyruvate, 2 mM glutamine, and 5% conditioned medium containing macrophage colony stimulating factor (M-CSF) produced by CMG cells to induce differentiation to BMDMs (Takeshita et al., 2000). BMDMs were differentiated for 6 days prior to harvesting and re-plating for experiments, and medium was changed at Day 4 of differentiation.

METHOD DETAILS

Cell Culture—For experiments using the H1299 *shCON* line without induction, 13×10^3 cells per well were plated in 24-well dishes at t = −16 h and changed into 0.6 mL labeling medium at t = 0 h. Labeling media consisted of DMEM (no glucose, glutamine, or phenol red; Thermo Fisher) supplemented with 2% FBS, 100 U/mL penicillin, 100 μg/mL streptomycin, 10 mM HEPES, 2 μg/mL puromycin, 25 mM glucose, and 4 mM glutamine. The labeling media contained 10%, 20%, 30%, 40%, 50%, 60%, 70%, 80%, 90%, or 100% U-$^{13}C_6$-glucose and U-$^{13}C_5$-glutamine (Cambridge Isotope Laboratories). At t = 48 h, cells were collected for fatty acid analysis using guanidine HCl.

For experiments using primary human fibroblasts, cells were plated into 12-well dishes using labeling medium (300×10^3 cells and 1 mL medium per well). Labeling medium consisted of DMEM (no glucose, glutamine, or phenol red) supplemented with 5% FBS, 100 U/mL penicillin, 100 μg/mL streptomycin, 25 mM U-$^{13}C_6$-glucose, and 4 mM U-$^{13}C_5$-

glutamine. After three days, the cells were collected for fatty acid analysis using guanidine HCl.

For siRNA knockdown experiments, 20 pmol of siRNA were combined with 2 mL of Dharmafect 4 transfection reagent in 200 μL of Optimem I (Thermo Fisher) defined medium in each well of a 12-well dish. A reverse transfection was carried out with 70×10^3 parental H1299 cells per well in RPMI supplemented with 10% FBS, 100 U/mL penicillin, and 100 μg/mL streptomycin. 12 hours post-transfection, the medium was replaced with RPMI 1640 (no glucose; Thermo Fisher) supplemented with 2% FBS, 100 U/mL penicillin, 100 μg/mL streptomycin, and 11 mM U-$^{13}C_6$-glucose. After 24 h, cells were collected for RNA analysis using TRIzol (Thermo Fisher). After 48 h, cells were collected for fatty acid analysis using guanidine HCl.

For experiments measuring parental H1299 cells at isotopic and metabolic steady state, cells were cultured in DMEM (no glucose; Thermo Fisher) supplemented with 5% FBS, 100 U/mL penicillin, 100 μg/mL streptomycin, and 25 mM U-$^{13}C_6$-glucose. Medium was refreshed every 12 hours, and cells were passaged with trypsin-EDTA as necessary to maintain a sub-confluent state. After 5 days (approximately 5 cell divisions), the cells were collected for fatty acid analysis using trypsin-EDTA.

For experiments using H1299 *shCON* and *shSCAP* lines with induction, cells were induced in 10 cm plates at t = −48 h using DMEM supplemented with 10% FBS, 100 U/mL penicillin, 100 μg/mL streptomycin, 10 mM HEPES, 2 μg/mL puromycin, and 15 ng/mL doxycycline (Sigma-Aldrich). Cells were re-plated in 12-well dishes at t = −16 h (30×10^3 cells per well) using DMEM supplemented with 5% FBS, 100 U/mL penicillin, 100 μg/mL streptomycin, 10 mM HEPES, 2 μg/mL puromycin, and 15 ng/mL doxycycline. At t = 0 h, a set of replicate wells were counted on-plate, and the remaining wells were changed into 1 mL of labeling medium. Labeling medium consisted of DMEM (no glucose, glutamine, or phenol red) supplemented with 5% FBS, 100 U/mL penicillin, 100 μg/mL streptomycin, 10 mM HEPES, 2 μg/mL puromycin, 25 mM U-$^{13}C_6$-glucose, 4 mM U-$^{13}C_5$-glutamine, and 15 ng/mL doxycycline. At t = 48 h, cells were collected for RNA analysis using TRIzol or counted on-plate and collected for fatty acid analysis using guanidine HCl.

For experiments using murine BMDMs, at day 6 of differentiation (t = −48 h), macrophages were scraped, counted, and re-plated into 12-well dishes using BMDM culture medium (200×10^3 cells per well). At day 8 (t = 0 h), a set of replicate wells were counted on-plate then collected using guanidine HCl, while the remaining wells were changed into 1 mL of labeling medium containing no treatment, Pam3CSK4 (PAM3, 50 ng/mL; Invivogen), Poly(I:C) (PIC, 1000 ng/mL; Invivogen), LPS (50 ng/mL; Invivogen), or MHV-68 (MOI = 1; Ting-Ting Wu (UCLA)). Labeling medium consisted of DMEM (no glucose, glutamine, or phenol red) supplemented with 5% FBS, 100 U/mL penicillin, 100 mg/mL streptomycin, 25 mM U-$^{13}C_6$-glucose, 6 mM U-$^{13}C_5$-glutamine, and 5% conditioned medium containing macrophage colony stimulating factor (M-CSF) produced by CMG cells. At day 9 (t = 24 h), cells were collected in TRIzol for RNA analysis. At day 10 (t = 48 h), cells were counted on-plate and collected for fatty acid analysis using guanidine HCl.

Gene Expression Analysis—Cells were collected in TRIzol and RNA was extracted using manufacturer's protocols. cDNA was synthesized with High-Capacity cDNA Reverse Transcription kit (Applied Biosystems) as per manufacturer's instructions (700 ng/μL RNA per cDNA synthesis reaction). Quantitative PCR (qPCR) was conducted on the Roche LightCycler 480 using SYBR Green Master Mix (Kapa Biosciences) and 0.5 μmol/L primers. Relative expression values are normalized to control gene (*36B4*) and expressed in terms of linear relative mRNA values.

Cell Counting and Guanidine HCl Collection—Unless specified as counted on-plate, cells were counted using a Cellometer K2 (Nexcelom) after lifting from culture dishes. H1299 cells and primary human fibroblasts were counted using a 1:4 dilution of trypan blue (Thermo Fisher), while BMDMs were counted using a 1:1 dilution of acridine orange/propidium iodide (Thermo Fisher, VWR). When counting on-plate, 1.25 μM Calcein-AM (final concentration; Santa Cruz Biotechnologies) was added to each well and incubated for 15 minutes. The plates were then imaged on a Molecular Devices ImageXpress XL. 24 high magnification fluorescence images were captured for each well (11.9% of total well surface area) using a 10x objective (Nikon Plan Fluor, 0.3 NA). Cell number was assessed using MetaXpress Software with Powercore using the Multi-wavelength cell scoring module. For collection with guanidine HCl, cells were treated with 50 μL or 75 μL of 6 M aqueous guanidine HCl and transferred to glass tubes for derivatization with an additional 100 μL or 150 μL of 3 M methanolic guanidine HCl (24-well plates and 12-well plates, respectively). Samples were prepared alongside internal standard curve samples made up of FAMEs (Nu-Chek Prep).

Lipid Derivatization and GC-MS—For experiments using the H1299 *shCON* line without induction and for the siRNA experiments, fatty acid methyl esters (FAMEs) were prepared as described previously (York et al., 2015).

For experiments using the parental H1299 line at isotopic and metabolic steady state, FAMEs were prepared as described previously (Ichihara and Fukubayashi, 2010) with the following modifications. After derivatization, 2 mL of aqueous 0.04 N NaCl was added to each sample. FAMEs were then extracted twice with 2 mL of hexane. The combined organic layers were then dried (EZ-2 Elite) and reconstituted in 100 μL of hexane for GC-MS analysis.

For all other experiments, FAMEs were prepared as described previously (Argus et al., 2017) with the following modifications. The final reaction volume of 725 μL contained 10.5% acetyl chloride, 10% toluene, and 6% water in methanol (v/v). The reaction proceeded at 45°C for 24 h, and was neutralized with 775 μL of 0.87M sodium carbonate in water. After addition of 1 mL of hexane, inversion, and centrifugation, the organic layer was extracted and dried. The remaining FAMEs were redissolved in 250 μL of hexane for analysis by GC-MS.

An Agilent 7890A-5975C GC-MS was used for analyzing the parental H1299 line at isotopic and metabolic steady state; an Agilent 7890B-5977A GC-MS was used for all other experiments. Complete GC-MS configurations and running programs are available upon

request. Integration and quantification of all ions was performed on MassHunter Quantitative Analysis Program (Agilent Technologies, B.06.00). Fatty acid pool sizes were determined by taking the sum of the area under the curve (AUC) for all isotopologues of the molecular ion, normalizing to internal standard (19:0 methyl ester added before derivatization; Nu-Chek Prep), and comparing to a FAMEs internal standard curve.

FAMEs Identification and Quantitation—The FAMEs standards used in these studies were the GLC-96 mix, 18:1n-7, and 19:0 (Nu-Chek Prep). FAMEs in biological samples were identified by molecular ion m/z (unit mass) and retention time compared to known standards. The only exception to this was two 20:1 isomers (distinct from 20:1n-9) in experiments related to Figures 5, 6, and 7 and S12. These analytes were identified as 20:1 isomers by molecular ion m/z (unit mass) and the proximity of their retention times to that of the 20:1n-9 standard. In these applications of FASA (Figures 5, 6, and 7 and S12), all 20:1 isomers were binned because specific isomer identification was unnecessary.

Given the large number of isotopologues quantified for each fatty acid, some at low abundance, it is possible that automated peak integration would quantify contaminants instead of or in addition to target compounds. To minimize the likelihood of this type of error in our isotopologue distributions, we visually inspected relevant extracted ion chromatogram peaks for every fatty acid in each sample, mock reaction, and calibration curve point to find and exclude potential contaminants whenever possible. In the rare case of coeluting contaminants, specific isotopologues were either flattened to zero (when the contaminant dwarfs a low abundance isotopologue) or not changed (when removal of the entire isotopologue affects the distribution more than the inclusion of the contaminant). SFA and MUFA isotopologues were normally collected up to M+(N+1), where N is the number of carbons in the fatty acid. In Figures 4 and S6, some fatty acids were collected up to M+N, M+(N-1), or M+(N-2). Given the very low predicted abundance at these ions, we do not anticipate their exclusion changes the results in any significant way. PUFA isotopologues were collected up to M+4 or M+6, depending on the fatty acid and experiment.

Correction for Natural Isotope Abundance—Correction for natural isotope abundance was performed using a matrix-based “skewed” correction algorithm (Midani et al., 2017) developed in-house. The following values were used for the natural abundance of stable isotopes: $^{1}H = 0.999885$, $^{2}H = 0.000115$, $^{12}C = 0.9893$, $^{13}C = 0.0107$, $^{16}O = 0.99757$, $^{17}O = 0.00038$, $^{18}O = 0.00205$ (Midani et al., 2017). The following carbon abundances were used for stable isotope labeled metabolites according to manufacturer information: $^{12}C = 0.01$, $^{13}C = 0.99$. Correction was applied to raw AUC values, and negative values were flattened to 0 (Moseley, 2010). For the ISA versus FASA comparisons (Figures 1, 2, S1–S5), the ELOVL1 knockdown (Figure S6), and the initial PUFA figures (Figures 3, S7), all isotope corrections (carbon, hydrogen, and oxygen) were performed before ISA and FASA analysis (including correction for ^{12}C in stable isotope-labeled metabolites). In all other figures, isotope corrections for hydrogen and oxygen were performed before FASA analysis and carbon isotopes (both ^{13}C from naturally occurring metabolites and ^{12}C in stable isotope-labeled metabolites) were accounted for as part of FASA analysis (see parameters q and e below).

Application of convISA—MATLAB .p files for convISA (Tredwell and Keun, 2015) were graciously shared by Dr. Hector Keun. Additional code was generated in-house to facilitate data input and output. The two parameter setting ("D" and "g(t)") was used for 14:0 and the three parameter setting (including a distribution for imported-elongated once, "elong") was used for other fatty acids. Other user-defined parameters were as follows: AcCoAlabels = 2, deriv = 'me', raw = 0, weighted = 0, CI = 0, x0 = [.5,.05,.2].

Fatty Acid Source Analysis - FASA—In utilizing FASA, an isotope of carbon (^{13}C) must be used as the label atom. In this paper, all isotopologue distribution data came from FAMEs. When isotopologue distribution data comes from FAMEs, all non-carbon natural isotope abundances must be corrected for before application of FASA, while all carbon natural isotope abundances (for label and natural carbons) can be corrected for before application of FASA or accounted for during the application of FASA. Note that if all carbon natural isotope abundances are corrected before using FASA, parameters q and e (see below for definitions) should be should be set at 0 and 1, respectively, when applying FASA.

In FASA, the total isotopologue distribution of a fatty acid with N total carbons, F_N, is modeled as a weighted mixture of multinomial distributions: fully synthesized, C_N, imported, B_N, and several imported-elongated distributions, $E_{N,i}$ (Equation 1).

$$F_N(n \mid q, \vec{S}, \vec{D}) = S * C_N(n \mid \vec{D}) + I * B_N(n \mid q) + \sum_{i=1}^{M} IE_i * E_{N,i}(n \mid i, q, \vec{D}) \quad \text{(Equation 1)}$$

The synthesized, imported, and imported-elongated multinomial distributions are functions of the ^{13}C abundance in natural metabolites (q), the isotopologue distribution of lipogenic acetyl-CoA ($\vec{D}$), and for imported-elongated distributions, the number of elongations (i). The parameter q can be set *a priori* or can be calculated from control cell lines grown with unlabeled media using maximum likelihood estimates. The multinomial distributions are scaled using the relative abundance of each fatty acid source ($\vec{S}$, Equation 2) and summed to produce the total isotopologue distribution F_N.

$$\vec{S} = [S, I, IE_1, \ldots, IE_M], \text{ where } M = \frac{N-14}{2} \quad \text{(Equation 2)}$$

S and I represent the proportion of a fatty acid pool that is fully synthesized and imported, respectively. IE_i represents the proportion of a fatty acid pool that results from shorter imported fatty acids that have been elongated by i acetyl-CoAs. In this model, we do not consider elongation of fatty acids shorter than myristate (14:0). Small corrections are made to account for the possible incorporation of ^{13}C in the methylation of fatty acids in GC-MS processing using q.

To account for the possibility of label diffusion, the isotopologue distribution of the lipogenic acetyl-CoA pool is directly modeled, with D_0, D_1, and D_2 representing the relative abundance of acetyl-CoAs containing 0, 1, or 2 ^{13}Cs (Equation 3).

$$\overrightarrow{D} = [D_0, D_1, D_2] \quad \text{(Equation 3)}$$

Note that if all carbon natural isotope abundances (for label and natural carbons) have been corrected for before application of FASA, $\overrightarrow{D}$ represents the carbon natural isotope abundance-corrected lipogenic acetyl-CoA pool.

D, the percent contribution of ^{13}C-labeled metabolites to the lipogenic acetyl-CoA pool, can be calculated as follows (Equation 4).

$$D = \frac{.5D_1 + D_2 - q}{e - q} \quad \text{(Equation 4)}$$

Parameter e represents the ^{13}C enrichment for each labeled metabolite used and is known *a priori*. This equation is valid when all labeled metabolites are uniformly labeled.

Imported fatty acids can be modeled as a binomial with N trials and success rate q, $B_N(n|q)$, as each carbon has an independent probability q of being ^{13}C. Because synthesized fatty acids are built using 2-carbon blocks of acetyl-CoA, that distribution is modeled as a sum of $N/2$ 2-carbon-units, each described as i.i.d. random variables $A(\overrightarrow{D})$ (Equation 5).

$$C_N(\overrightarrow{D}) = \sum_{1}^{\frac{N}{2}} [A(\overrightarrow{D})], \text{ where } A(n \mid \overrightarrow{D}) = \begin{cases} D_0 \text{ if } n = 0 \\ D_1 \text{ if } n = 1 \\ D_2 \text{ if } n = 2 \end{cases} \quad (5)$$

The multinomial distribution of an N-carbon fatty acid after undergoing i elongations, $E_{N,i}$, is the sum of the binomial distribution of the imported FA, and a "synthesized" distribution of i acetyl-CoAs (Equation 6).

$$E_{N,i}(i, q, \overrightarrow{D}) = B_{N-2*i}(q) + C_{i*2}(\overrightarrow{D}) \quad \text{(Equation 6)}$$

Based on this model, our distributions are defined by the (M+6)x1 parameter vector $\overrightarrow{B} = [q, D_0, D_1, D_2, S, I, IE_1, \ldots IE_M]$. Note that because the elements of $\overrightarrow{S}$ and $\overrightarrow{D}$ each must sum to 1, optimizations must be constrained. We enforce this constraint as follows (Equations 7 and 8):

$$D_2 = 1 - D_0 - D_1 \quad \text{(Equation 7)}$$

$$IE_M = 1 - S - I - \sum_{i=1}^{M-1} IE_i \quad \text{(Equation 8)}$$

Therefore, optimizations are performed over the (M+4)x1 parameter vector $\vec{b} = [q, D_0, D_1, S, I, IE_1, \ldots IE_{\text{M-1}}]$. Maximum likelihood estimates are acquired for $\vec{b}$, using a modified gradient descent algorithm. To ensure convergence to the global maximum instead of local maxima, each dataset is fit multiple times with random initial conditions.

In addition, this model allows for fixing parameter elements of $\vec{b}$ which are known *a priori*, and will not be fit by the iterative algorithm. The most common parameter to fix will be background ^{13}C abundance (q). We also allow for $\vec{D}$ and any element of $\vec{S}$ to be fixed based on data or *a priori* knowledge of metabolic pathways; this allows extension of FASA to fatty acids with little or no synthesis. Note that when fixing elements of $\vec{S}$, the rightmost element of $\vec{S}$ which is not held constant is constrained such that the elements of $\vec{S}$ sum to 1.

If label diffusion is assumed to be zero, $\vec{D}$ can be simplified to D and $1\text{-}D$. To accomplish this, D_1 and D_2 become functions of D_0, q, and e as follows (Equations 9–11):

$$D_1 = (1 - D)[2q(1 - q)] + (D)[2e(1 - e)] \quad \text{(Equation 9)}$$

$$D_2 = 1 - D_0 - D_1 \quad \text{(Equation 10)}$$

$$\text{Where } D = \frac{D_0 - (1 - q)^2}{(1 - e)^2 - (1 - q)^2} \quad \text{(Equation 11)}$$

Note that if FASA is constrained to disallow label diffusion, all labeled metabolites used must be uniformly labeled.

***In silico* Tests of FASA—**To test the robustness of FASA to variations in input data and noise, we performed *in silico* tests on the model. 14-to 24-carbon fatty acids with the possibility of *de novo* synthesis (representing SFA and MUFA) were tested independently. To test D, realistic parameter sets for fatty acid sources were chosen for each fatty acid length (based on empirical data, see Table S5 for values) while D was varied between 5%–

80% (assuming no label diffusion). To test S, realistic parameter sets for D_0, D_1, D_2, and fatty acid sources were chosen for each fatty acid length (based on empirical data, see Table S5 for values) while S was varied from 1%–90%, depending on observed ranges for each fatty acid. As S varied, I responded, while the IE parameters were kept constant. To test IE_{max} (the IE parameter with the most elongations), realistic parameter sets for D_0, D_1, D_2, and fatty acid sources were chosen for each fatty acid (based on empirical data, see Table S5 for values) while IE_{max} was varied from 0.1%–8%. As IE_{max} varied, S responded, while I and the remaining IE parameters were kept constant.

For each theoretical isotopologue distribution, 25 realizations of Gaussian noise were simulated at two noise levels (2% or 10% relative standard deviation – see "Confidence Interval Determination" section below for additional information on the choice of these values). Each of these "noisy" datasets was then analyzed independently by FASA. "Bias" represents the average of the percent errors between the fitted parameter values and the true parameter value. "RSD" represents the relative standard deviation of the fitted parameter values.

Steady State and FASA Parameter Definitions—We define metabolic steady state (mSS) as the point at which per cell fluxes and pool sizes for a given metabolite remain constant for the average cell in a population (Buescher et al., 2015). We define isotopic steady state (iSS) as the point at which the isotopologue distribution remains constant for a given metabolite (Buescher et al., 2015). mSS and iSS for fatty acids can be approximated by culturing cells in a sub-confluent state in stable isotope-labeled media for a period of time that is sufficient for the original fatty acids to be diluted out (Buescher et al., 2015; Metallo et al., 2011). In an idealized system (mSS, no fatty acid losses, acetyl-CoA pool reaches iSS within a few hours), 5 cell divisions is sufficient to dilute pre-existing fatty acid contribution to below 5%. In practice, losses may cause iSS to be reached more quickly.

For FASA at mSS and iSS, I represents the contribution of import for a given fatty acid. If fatty acid shortening is non-negligible, I will be a mixture of directly imported fatty acid and imported-shortened fatty acid.

Variable FASN Products—Though the final product of FASN is primarily 16:0, it has been reported to produce 14:0 and 18:0 at lower frequency (Vance and Vance, 2008; Wakil, 1989). One challenge this creates is the inability of ISA and FASA to differentiate certain synthesized origins (e.g., a FASN-synthesized 18:0 from a FASN-synthesized 16:0 that is subsequently elongated). For simplicity, we assume that with the exception of the 14:0 pool, all FASN products are 16:0. As a result, at iSS and mSS, for 16:0 and 16:1n-7, IE_1 will be an underestimate of the contribution of elongation and S will be an overestimate for the contribution of synthesis. For 18:0 and 18:1n-9 at iSS and mSS, 1-I will overestimate the contribution of elongation. 18:1n-7 does not have this issue because it is a direct elongation product of 16:1n-7.

When applying FASA before fatty acid pools have reached iSS and mSS, calculation of the accumulation of FASN products will not be affected, as we assume that any molecule comprised of all carbons from the lipogenic acetyl CoA pool was synthesized by FASN

(regardless of whether the direct FASN product was 14:0, 16:0, or 18:0). The accumulation of 14 to 16 elongation products (SFA+MUFA) will be underestimated because our calculations do not include the elongation of FASN-synthesized 14:0. The accumulation of 16 to 18 elongation products (SFA+MUFA) will be overestimated because our calculations include direct FASN synthesis of 18:0.

Interpretation of D—In both ISA and FASA, *D* represents the percent contribution of ^{13}C-labeled metabolites to the lipogenic acetyl-CoA pool. We make the assumption that the lipogenic acetyl-CoA pool reaches iSS relatively quickly compared to total labeling time. One group demonstrated that ISA can be applied after 6 hours of labeling, with multiple relevant central carbon metabolites (including citrate) approaching isotopic steady state at or before 2 hours of labeling (Yoo et al., 2008). Furthermore, ISA is routinely applied after 24 hours of labeling (Green et al., 2016; Parker et al., 2017). As a result, we do not believe our application of FASA after 48 hours of labeling is problematic, and we anticipate that FASA could be applied after shorter periods of labeling as well.

Note that for both ISA and FASA, when the acetyl-CoA pool reaches iSS, *D* represents both direct and indirect contributions (e.g., ^{13}C glucose to ^{13}C amino acids to ^{13}C acetyl-CoA). In addition, the ratio of *D* to *1-D* represents the ratio of the fluxes of these two carbon sources into the lipogenic acetyl-CoA pool if it is assumed to be at iSS and that there is no preferential loss. Note that though *D* and *1-D* represent relative fluxes in this case, additional information would be needed to determine absolute fluxes. This is in part due to multiple fates of acetyl-CoA in the cell beyond fatty acid synthesis and elongation, including oxidation, prenol and sterol lipid synthesis, and protein acetylation (Vance and Vance, 2008).

Accumulation of FASN and Elongation Products—For accumulation of elongated 20:3n-6 and 22:4n-6 during the labeling period, the following formula was used (Equation 12).

$$A_x = \frac{P_x * (IE_{1,x} + IE_{2,x})}{c_{avg}} \quad \text{(Equation 12)}$$

A_x represents the accumulation of elongated fatty acid x during the labeling period. P_x represents the total amount of fatty acid x in the sample. $IE_{1,x}$ and $IE_{2,x}$ represent the FASA parameters IE_1 and IE_2 for fatty acid x. c_{avg} represents the average cell number during the labeling period and is calculated assuming exponential growth between starting and final cell counts (c_i and c_f, respectively) using the following formulae (Equation 13).

$$c_{avg} = \frac{c_i\theta\left(2^{\frac{t_f}{\theta}} - 2^{\frac{t_i}{\theta}}\right)}{\ln 2(t_f - t_i)}, \text{ where } \theta = \frac{t \ln 2}{\ln\frac{c_f}{c_i}} \quad \text{(Equation 13)}$$

Θ represents the exponential doubling time, and t_f and t_i represent final and initial times, respectively.

For saturated fatty acids (SFA) and monounsaturated fatty acids (MUFA), because data exists for a large number of fatty acids in a single pathway, one can go a step further and calculate the contribution of each pathway step to accumulated fatty acids. Note that SFA and MUFA of the same length were combined in this analysis because in general, the relevant elongases are similar (Sassa and Kihara, 2014; Vance and Vance, 2008). For a particular elongation step, we first determined all fatty acid origins that require having passed through that elongation step to exist (Figure 5B). All of the fatty acids measured and used in the accumulation experiments are listed in Table S5. Note that the 20:1 isotopologue distribution was a sum of three peaks; 20:1n-9 was identified using a standard, and the other two species were presumed to be 20:1n-11 and 20:1n-7 based on relative retention time and mass spectra. In this analysis, these fatty acids were binned as the location of the double bond does not affect our determinations of fatty acid source (synthesized, imported-elongated, and imported).

Multiplying the selected parameter values by the final amount of each fatty acid divided by the average cell number on the plate during labeling resulted in the contributions that each fatty acid made to the total accumulation of elongation products through a particular elongation step over the labeling period (Figure 5C). Summing these individual contributions gave the total accumulation of elongation products for a particular elongation step (nmol/1e6 cells) during the labeling period (Figure 5D). This process was the same for synthesis, except that only S for all fatty acid was used.

QUANTIFICATION AND STATISTICAL ANALYSIS

General Statistics—General statistical details of experiments can be found in figure legends (definition and value of n, definition of center and dispersion measures). Unless otherwise stated, statistical tests were performed using a two-tailed heteroscedastic Student's t test. ns (not significant) - $p \geq 0.05$; * - $0.01 \leq p < 0.05$; ** - $0.001 \leq p < 0.01$; *** - $p < 0.001$.

Log-Likelihood Ratio Test—The log-likelihood ratio test (LLRT) was used to compare the goodness of fit between FASA and ISA, as ISA can be considered to be a special case of FASA. p values were determined using the test statistic T and the right-tailed chi-square distribution with degrees of freedom f as defined below (Equation 14).

$$T = 2[LogL(FASA) - LogL(ISA)] = 2\left[\frac{SSE_{ISA}}{2\sigma^2} - \frac{SSE_{FASA}}{2\sigma^2}\right],\ f = m_{FASA} - m_{ISA} \quad \text{(Equation 14)}$$

SSE_n represents the sum of squared errors for the best fit using model n. σ represents the standard deviation of the measurement error of the individual isotopologues in a normalized isotopologue distribution (a measurement of instrument noise). m_n represents the number of parameters in model n.

In our analysis using LLRTs, we have assumed a uniform error structure (N(0,σ)) across isotopologues and estimated σ as < 0.4% from 20 injections of the same FAMEs standard (using the 7890A-5975C GC-MS). This simplified method is not a perfect representation of the true error structure, as rare isotopologues have smaller variances than common isotopologues. However, the imperfections this brings into p value calculations for the LLRT should be minimal. As the ISA model generally performs better in fitting common isotopologues, and fails at fitting rare species fit well by the FASA model, the error structure we assume under-penalizes ISA's poor fitting of rare species. Therefore, using a more complex, but more accurate, error structure would likely lead to more significant results than are reported in this work.

Confidence Interval Calculation—Confidence intervals for parameter fits we estimated using the following equation (Equation 15):

$$\sigma_p = \sqrt{diag\left([J^T W J]^{-1}\right)} \quad \text{(Equation 15)}$$

Where σ_p is a vector of the estimated SDs of the fitted parameters, J is the Jacobian of the optimization function at the final iteration, and W is a weighting matrix, where $W_{ii} = 1 / \sigma_i^2$, the inverse of the variance of ith measured isotopologue, y_i. In the LLRT, a constant σ_i was used because as true error structure cannot be known, and using constant σ_i provides a more conservative estimate of significance (see above). However, using a constant σ_i for confidence interval calculation would lead to highly inaccurate results. Therefore, we were forced to modify our estimated error structure. Data from 20 repeated injections of a FAMEs standard mix showed that there was a roughly linear relationship between σ_i and AUC_i for each y_i, which therefore lead us to estimate the relative σ_i (RSD) of 1.67% for all y_i. We calculated confidence intervals assuming several values for relative σ_i (RSD) including 2%, 5%, and 10% to control for possible errors in RSD estimation.

DATA AND SOFTWARE AVAILABILITY

Availability of FASA Code—Source code for FASA is available at https://github.com/BensingerLab/FASA.

Supplementary Material

Refer to Web version on PubMed Central for supplementary material.

ACKNOWLEDGMENTS

This work was supported in part by National Institute of General Medical Sciences grant T32 GM008469 (to J.P.A.), National Institute of Allergy and Infectious Diseases grant AI093768 (to S.J.B.), and National Heart, Lung,

and Blood Institute grant HL126556 (to S.J.B.). Other support was provided by the UCLA Graduate Division and the UCLA Dissertation Year Fellowship (to J.P.A.). The content is solely the responsibility of the authors and does not necessarily represent the official views of the NIH. We wish to thank Dr. Harvey Herschman (UCLA) for providing 293FT cells, Dr. Andrew Aplin (Thomas Jefferson University) for providing pLentipuro/BLOCK-iT-DEST, Dr. Diane M. Simeone (University of Michigan) for providing pLenti0.3/EF/GW/IVS-Kozak-TetR-P2A-Bsd, and Dr. Ting-Ting Wu (UCLA) for providing MHV-68. We wish to thank Dr. Hector Keun (Imperial College London) for providing the code for convISA. We also thank Drs. James Wohlschlegel and Ajit Divakaruni (UCLA) for providing thoughtful analysis.

REFERENCES

Abel EV, Basile KJ, Kugel CH, 3rd, Witkiewicz AK, Le K, Amaravadi RK, Karakousis GC, Xu X, Xu W, Schuchter LM, et al. (2013). Melanoma adapts to RAF/MEK inhibitors through FOXD3-mediated upregulation of ERBB3. J. Clin. Invest. 123, 2155–2168. [PubMed: 23543055]

Argus JP, Yu AK, Wang ES, Williams KJ, and Bensinger SJ (2017). An optimized method for measuring fatty acids and cholesterol in stable isotope-labeled cells. J. Lipid Res. 58, 460–468. [PubMed: 27974366]

Buescher JM, Antoniewicz MR, Boros LG, Burgess SC, Brunengraber H, Clish CB, DeBerardinis RJ, Feron O, Frezza C, Ghesquiere B, et al. (2015). A roadmap for interpreting (13)C metabolite labeling patterns from cells. Curr. Opin. Biotechnol. 34, 189–201. [PubMed: 25731751]

Bulusu V, Tumanov S, Michalopoulou E, van den Broek NJ, MacKay G, Nixon C, Dhayade S, Schug ZT, Vande Voorde J, Blyth K, et al. (2017). Acetate Recapturing by Nuclear Acetyl-CoA Synthetase 2 Prevents Loss of Histone Acetylation during Oxygen and Serum Limitation. Cell Rep. 18, 647–658. [PubMed: 28099844]

Collins JM, Neville MJ, Pinnick KE, Hodson L, Ruyter B, van Dijk TH, Reijngoud D-J, Fielding MD, and Frayn KN (2011). De novo lipogenesis in the differentiating human adipocyte can provide all fatty acids necessary for maturation. J. Lipid Res. 52, 1683–1692. [PubMed: 21677304]

Divakaruni AS, Hsieh WY, Minarrieta L, Duong TN, Kim KKO, Desousa BR, Andreyev AY, Bowman CE, Caradonna K, Dranka BP, et al. (2018). Etomoxir Inhibits Macrophage Polarization by Disrupting CoA Homeostasis. Cell Metab. 28, 490–503.e7. [PubMed: 30043752]

Gelman SJ, Naser F, Mahieu NG, McKenzie LD, Dunn GP, Chheda MG, and Patti GJ (2018). Consumption of NADPH for 2-HG Synthesis Increases Pentose Phosphate Pathway Flux and Sensitizes Cells to Oxidative Stress. Cell Rep. 22, 512–522. [PubMed: 29320744]

Green CR, Wallace M, Divakaruni AS, Phillips SA, Murphy AN, Ciaraldi TP, and Metallo CM (2016). Branched-chain amino acid catabolism fuels adipocyte differentiation and lipogenesis. Nat. Chem. Biol. 12, 15–21. [PubMed: 26571352]

Hellerstein MK, and Neese RA (1992). Mass isotopomer distribution analysis: a technique for measuring biosynthesis and turnover of polymers. Am. J. Physiol. 263, E988–E1001. [PubMed: 1443132]

Horton JD, Goldstein JL, and Brown MS (2002). SREBPs: activators of the complete program of cholesterol and fatty acid synthesis in the liver. J. Clin. Invest. 109, 1125–1131. [PubMed: 11994399]

Ichihara K, and Fukubayashi Y (2010). Preparation of fatty acid methyl esters for gas-liquid chromatography. J. Lipid Res. 51, 635–640. [PubMed: 19759389]

Jonas MC, Pehar M, and Puglielli L (2010). AT-1 is the ER membrane acetyl-CoA transporter and is essential for cell viability. J. Cell Sci. 123, 3378–3388. [PubMed: 20826464]

Kelleher JK, and Masterson TM (1992). Model equations for condensation biosynthesis using stable isotopes and radioisotopes. Am. J. Physiol. 262, E118–E125. [PubMed: 1733242]

Kelleher JK, and Nickol GB (2015). Isotopomer Spectral Analysis: Utilizing Nonlinear Models in Isotopic Flux Studies. Methods Enzymol. 561, 303–330. [PubMed: 26358909]

Koyuncu E, Purdy JG, Rabinowitz JD, and Shenk T (2013). Saturated very long chain fatty acids are required for the production of infectious human cytomegalovirus progeny. PLoS Pathog. 9, e1003333. [PubMed: 23696731]

Krämer L, Jäger C, Trezzi J-P, Jacobs DM, and Hiller K (2018). Quantification of Stable Isotope Traces Close to Natural Enrichment in Human Plasma Metabolites Using Gas Chromatography-Mass Spectrometry. Metabolites 8, 15.

Lau CE, Tredwell GD, Ellis JK, Lam EW-F, and Keun HC (2017). Metabolomic characterisation of the effects of oncogenic PIK3CA transformation in a breast epithelial cell line. Sci. Rep. 7, 46079. [PubMed: 28393905]

Le HD, Meisel JA, de Meijer VE, Gura KM, and Puder M (2009). The essentiality of arachidonic acid and docosahexaenoic acid. Prostaglandins Leukot. Essent. Fatty Acids 81, 165–170. [PubMed: 19540099]

Lee WN, Bassilian S, Guo Z, Schoeller D, Edmond J, Bergner EA, and Byerley LO (1994a). Measurement of fractional lipid synthesis using deuterated water (2H2O) and mass isotopomer analysis. Am. J. Physiol. 266, E372–E383. [PubMed: 8166257]

Lee WN, Bassilian S, Ajie HO, Schoeller DA, Edmond J, Bergner EA, and Byerley LO (1994b). In vivo measurement of fatty acids and cholesterol synthesis using D2O and mass isotopomer analysis. Am. J. Physiol. 266, E699–E708. [PubMed: 8203508]

Lligona-Trulla L, Arduini A, Aldaghlas TA, Calvani M, and Kelleher JK (1997). Acetyl-L-carnitine flux to lipids in cells estimated using isotopomer spectral analysis. J. Lipid Res. 38, 1454–1462. [PubMed: 9254070]

Matsuda M, Korn BS, Hammer RE, Moon YA, Komuro R, Horton JD, Goldstein JL, Brown MS, and Shimomura I (2001). SREBP cleavage-activating protein (SCAP) is required for increased lipid synthesis in liver induced by cholesterol deprivation and insulin elevation. Genes Dev. 15, 1206–1216. [PubMed: 11358865]

Metallo CM, Gameiro PA, Bell EL, Mattaini KR, Yang J, Hiller K, Jewell CM, Johnson ZR, Irvine DJ, Guarente L, et al. (2011). Reductive glutamine metabolism by IDH1 mediates lipogenesis under hypoxia. Nature 481, 380–384. [PubMed: 22101433]

Midani FS, Wynn ML, and Schnell S (2017). The importance of accurately correcting for the natural abundance of stable isotopes. Anal. Biochem. 520, 27–43. [PubMed: 27989585]

Moseley HNB (2010). Correcting for the effects of natural abundance in stable isotope resolved metabolomics experiments involving ultra-high resolution mass spectrometry. BMC Bioinformatics 11, 139. [PubMed: 20236542]

O'Neill LAJ, and Pearce EJ (2016). Immunometabolism governs dendritic cell and macrophage function. J. Exp. Med. 213, 15–23. [PubMed: 26694970]

Oosterveer MH, van Dijk TH, Tietge UJF, Boer T, Havinga R, Stellaard F, Groen AK, Kuipers F, and Reijngoud D-J (2009). High fat feeding induces hepatic fatty acid elongation in mice. PLoS ONE 4, e6066. [PubMed: 19557132]

Parker SJ, Svensson RU, Divakaruni AS, Lefebvre AE, Murphy AN, Shaw RJ, and Metallo CM (2017). LKB1 promotes metabolic flexibility in response to energy stress. Metab. Eng. 43 (Pt B), 208–217. [PubMed: 28034771]

Sassa T, and Kihara A (2014). Metabolism of very long-chain Fatty acids: genes and pathophysiology. Biomol. Ther. (Seoul) 22, 83–92. [PubMed: 24753812]

Stein SE (1999). An integrated method for spectrum extraction and compound identification from gas chromatography/mass spectrometry data. J. Am. Soc. Mass Spectrom. 10, 770–781.

Takeshita S, Kaji K, and Kudo A (2000). Identification and characterization of the new osteoclast progenitor with macrophage phenotypes being able to differentiate into mature osteoclasts. J. Bone Miner. Res. 15, 1477–1488. [PubMed: 10934646]

Tredwell GD, and Keun HC (2015). convISA: A simple, convoluted method for isotopomer spectral analysis of fatty acids and cholesterol. Metab. Eng. 32, 125–132. [PubMed: 26432945]

Vance DE, and Vance JE (2008). Biochemistry of Lipids, Lipoproteins and Membranes (Oxford, UK: Elsevier B.V.).

Wakil SJ (1989). Fatty acid synthase, a proficient multifunctional enzyme. Biochemistry 28, 4523–4530. [PubMed: 2669958]

Wong DA, Bassilian S, Lim S, and Paul Lee W-N (2004). Coordination of peroxisomal beta-oxidation and fatty acid elongation in HepG2 cells. J. Biol. Chem. 279, 41302–41309. [PubMed: 15277519]

Yao CH, Fowle-Grider R, Mahieu NG, Liu GY, Chen YJ, Wang R, Singh M, Potter GS, Gross RW, Schaefer J, et al. (2016). Exogenous Fatty Acids Are the Preferred Source of Membrane Lipids in Proliferating Fibroblasts. Cell Chem. Biol. 23, 483–493. [PubMed: 27049668]

Yoo H, Antoniewicz MR, Stephanopoulos G, and Kelleher JK (2008). Quantifying reductive carboxylation flux of glutamine to lipid in a brown adipocyte cell line. J. Biol. Chem. 283, 20621–20627. [PubMed: 18364355]

York AG, Williams KJ, Argus JP, Zhou QD, Brar G, Vergnes L, Gray EE, Zhen A, Wu NC, Yamada DH, et al. (2015). Limiting Cholesterol Biosynthetic Flux Spontaneously Engages Type I IFN Signaling. Cell 163, 1716–1729. [PubMed: 26686653]

Zhang C, Wang Y, Wang F, Wang Z, Lu Y, Xu Y, Wang K, Shen H, Yang P, Li S, et al. (2017). Quantitative profiling of glycerophospholipids during mouse and human macrophage differentiation using targeted mass spectrometry. Sci. Rep. 7, 412. [PubMed: 28341849]

Highlights

- Fatty Acid Source Analysis (FASA) quantifies fatty acid synthesis, elongation, and import
- FASA improves previous models by including multiple imported-elongated fatty acids
- Elongation can be a major contributor to cellular fatty acid content
- Different stimuli reprogram macrophage fatty acid elongation in distinct ways

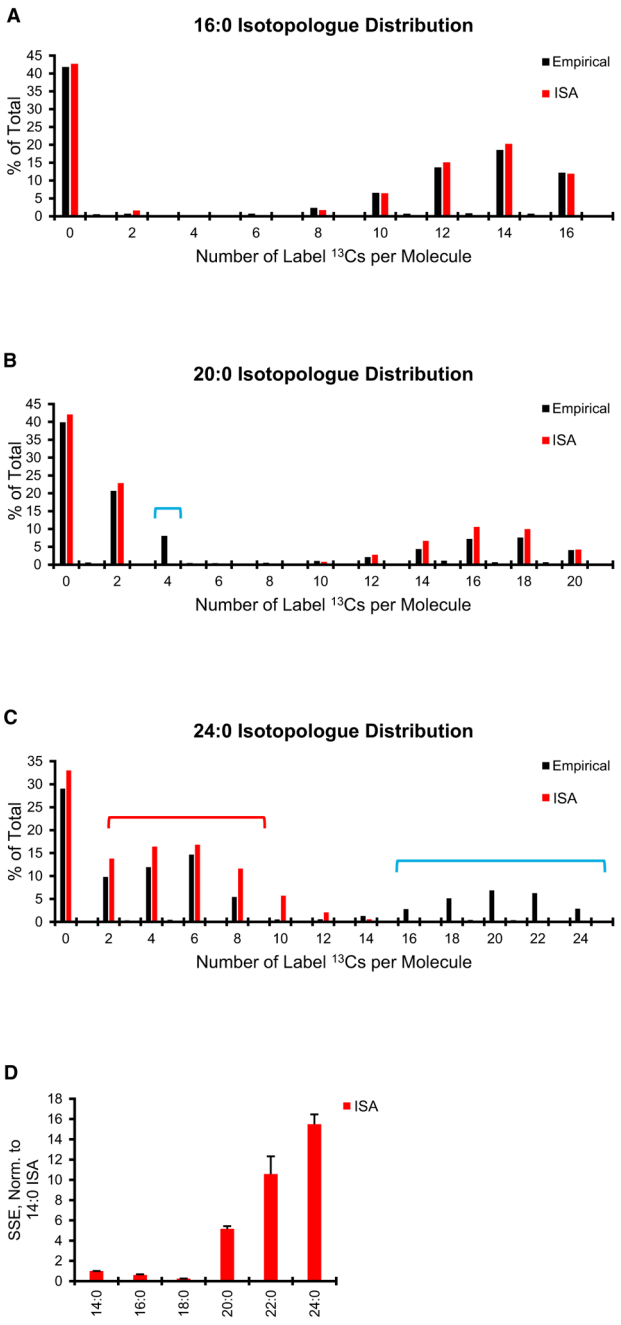

Figure 1. ISA Yields Suboptimal Fits for Fatty Acids Containing 20–24 Carbons

H1299 *shCON* cells were cultured in medium containing 2% FBS, 100% U-$^{13}C_6$-glucose, and 100% U-$^{13}C_5$-glutamine. After 48 hr of labeling, cells were collected, and isotopologue distributions were determined for fatty acids.

(A–C) Representative empirical (black) and ISA-derived (red) isotopologue distributions for (A) 16:0, (B) 20:0, and (C) 24:0. The red bracket indicates overestimation of empirical data by ISA modeling, whereas the blue brackets indicate underestimation.

(D) ISA sum of squared error (SSE) for the indicated fatty acids normalized to 14:0 ISA.

The isotopologue distributions are representative singlets of biological quadruplicates and are corrected for natural abundance of C, H, and O isotopes. SSEs are the average ± SD of biological quadruplicates. See also Figures S1–S5.

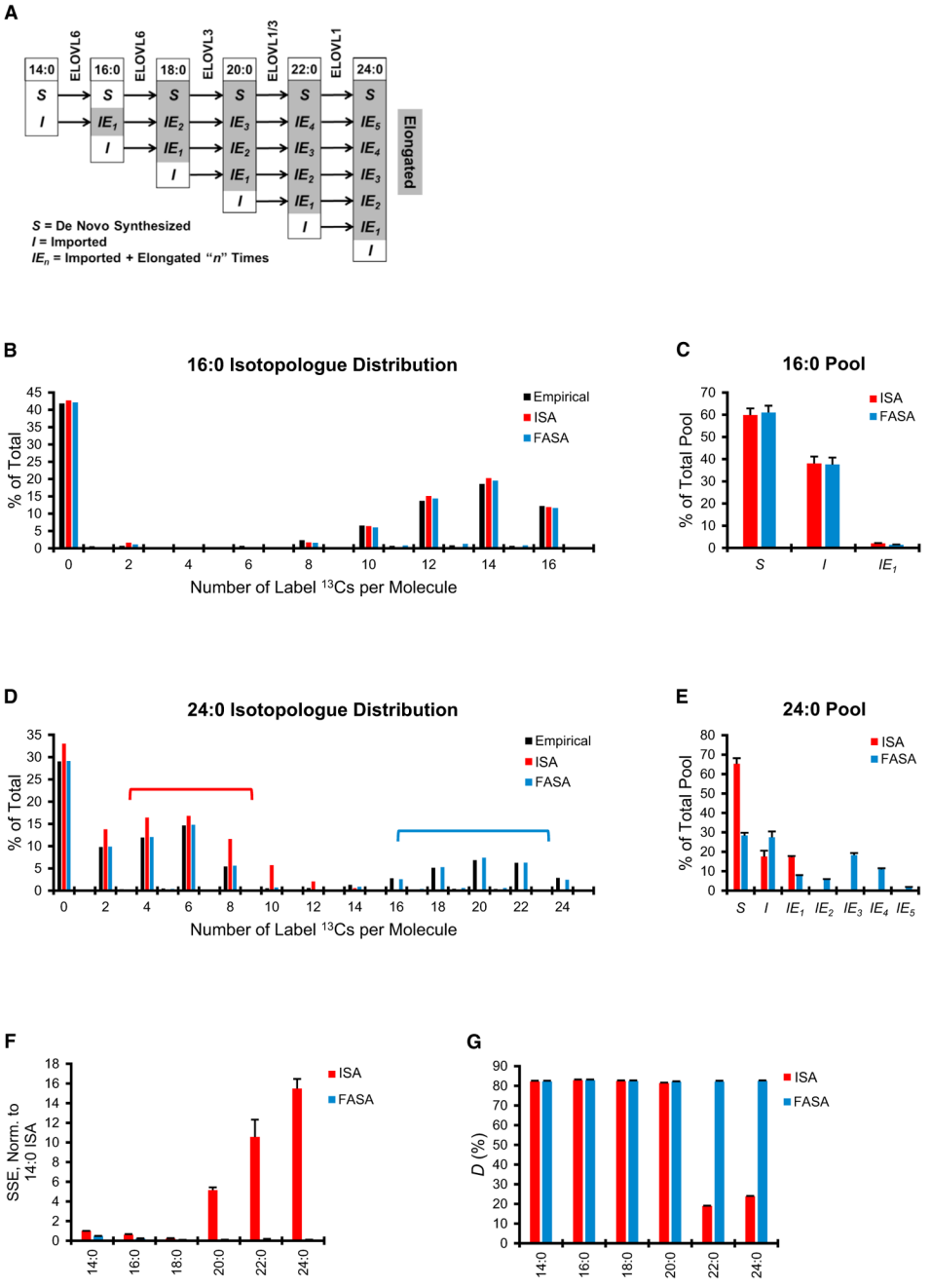

Figure 2. FASA Significantly Improves Fits for Fatty Acids Containing 20–24 Carbons

H1299 *shCON* cells were cultured in medium containing 2% FBS, 100% U-$^{13}C_6$-glucose, and 100% U-$^{13}C_5$-glutamine. After 48 hr of labeling, cells were collected, and isotopologue distributions were determined for fatty acids.

(A) Schematic of possible contributions to the indicated saturated fatty acids used by FASA. All parameters marked in gray are considered elongated (see STAR Methods for additional details). *S*, synthesized; *I*, imported; IE_n, imported and elongated *n* times.

(B) Representative empirical (black), ISA-derived (red), and FASA-derived (blue) isotopologue distributions for 16:0.

(C) Model-derived contribution parameters for the 16:0 pool.
(D) Representative empirical, ISA-derived, and FASA-derived isotopologue distributions for 24:0. The red bracket indicates overestimation of empirical data by ISA modeling, whereas the blue bracket indicates underestimation.
(E) Model-derived contribution parameters for the 24:0 pool.
(F) SSE for ISA and FASA, normalized to 14:0 ISA.
(G) Model-derived D (fractional contribution of ^{13}C-labeled metabolites to the lipogenic acetyl-CoA) for the indicated fatty acids using ISA or FASA.
The isotopologue distributions shown are representative singlets of biological quadruplicates and are corrected for natural abundance of C, H, and O isotopes. Data shown for pool contribution parameters, SSEs, and D are the average ± SD of biological quadruplicates. See also Figures S1–S6 and S8–S11 and Table S2.

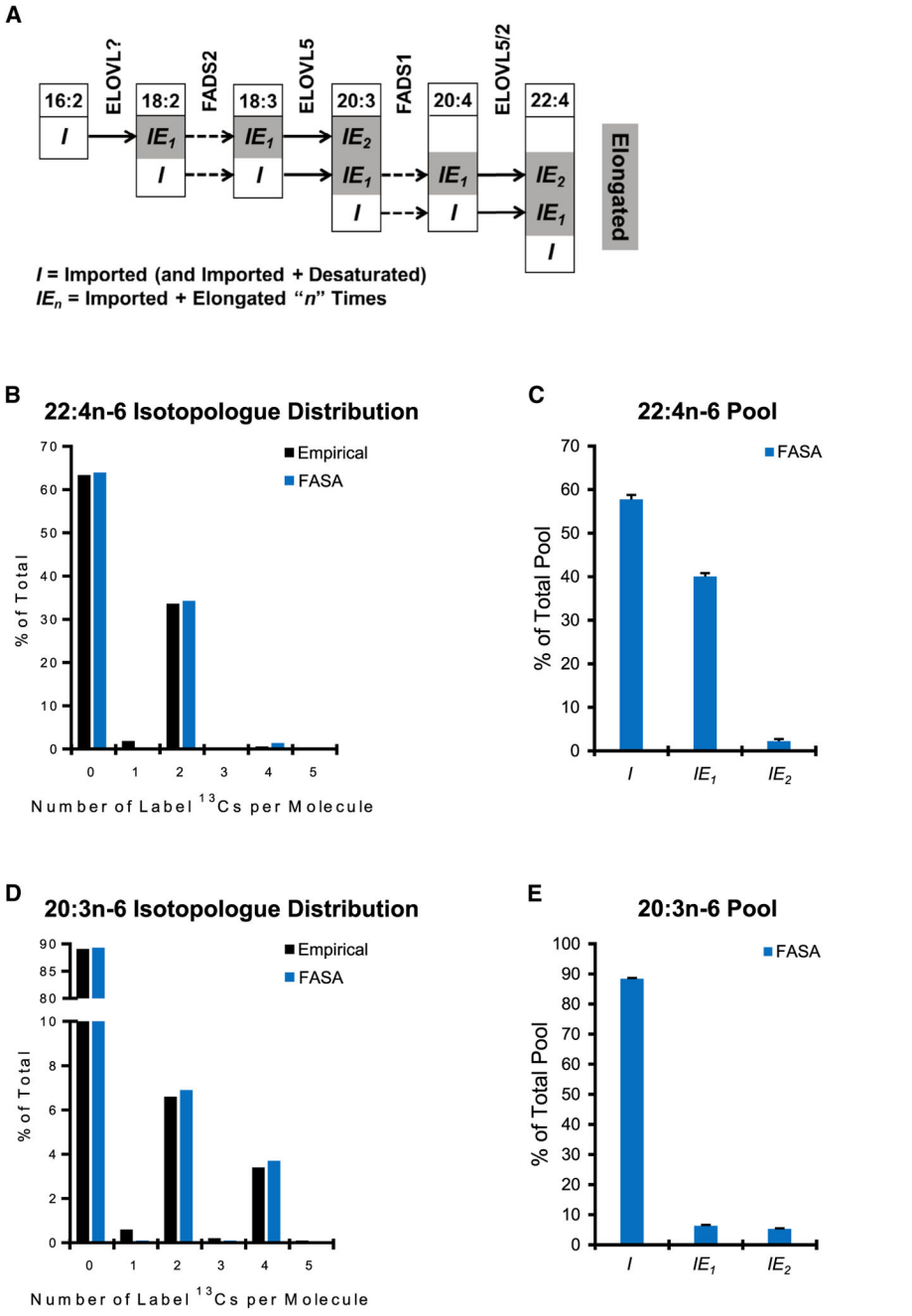

Figure 3. FASA Provides Good Fits for Polyunsaturated Fatty Acids

H1299 *shCON* cells were cultured in medium containing 2% FBS, 100% U-$^{13}C_6$-glucose, and 100% U-$^{13}C_5$-glutamine. After 48 hr of labeling, cells were collected, and isotopologue distributions were determined for fatty acids. When applying FASA to polyunsaturated fatty acids (PUFAs), values for D_0, D_1, and D_2 were fixed using results from 16:0 to facilitate modeling.

(A) Schematic of possible contributions to the indicated n-6 PUFAs used by FASA. All parameters marked in gray are considered elongated.

(B) Representative empirical isotopologue distribution and FASA modeling for 22:4n-6.

(C) FASA-derived contribution parameters for the 22:4n-6 pool.
(D) Representative empirical isotopologue distribution and FASA modeling for 20:3n-6.
(E) FASA-derived contribution parameters for the 20:3n-6 pool.
The isotopologue distributions shown are representative singlets of biological quadruplicates and are corrected for natural abundance of C, H, and O isotopes. Data shown for pool contribution parameters are the average ± SD of biological quadruplicates. See also Figure S7.

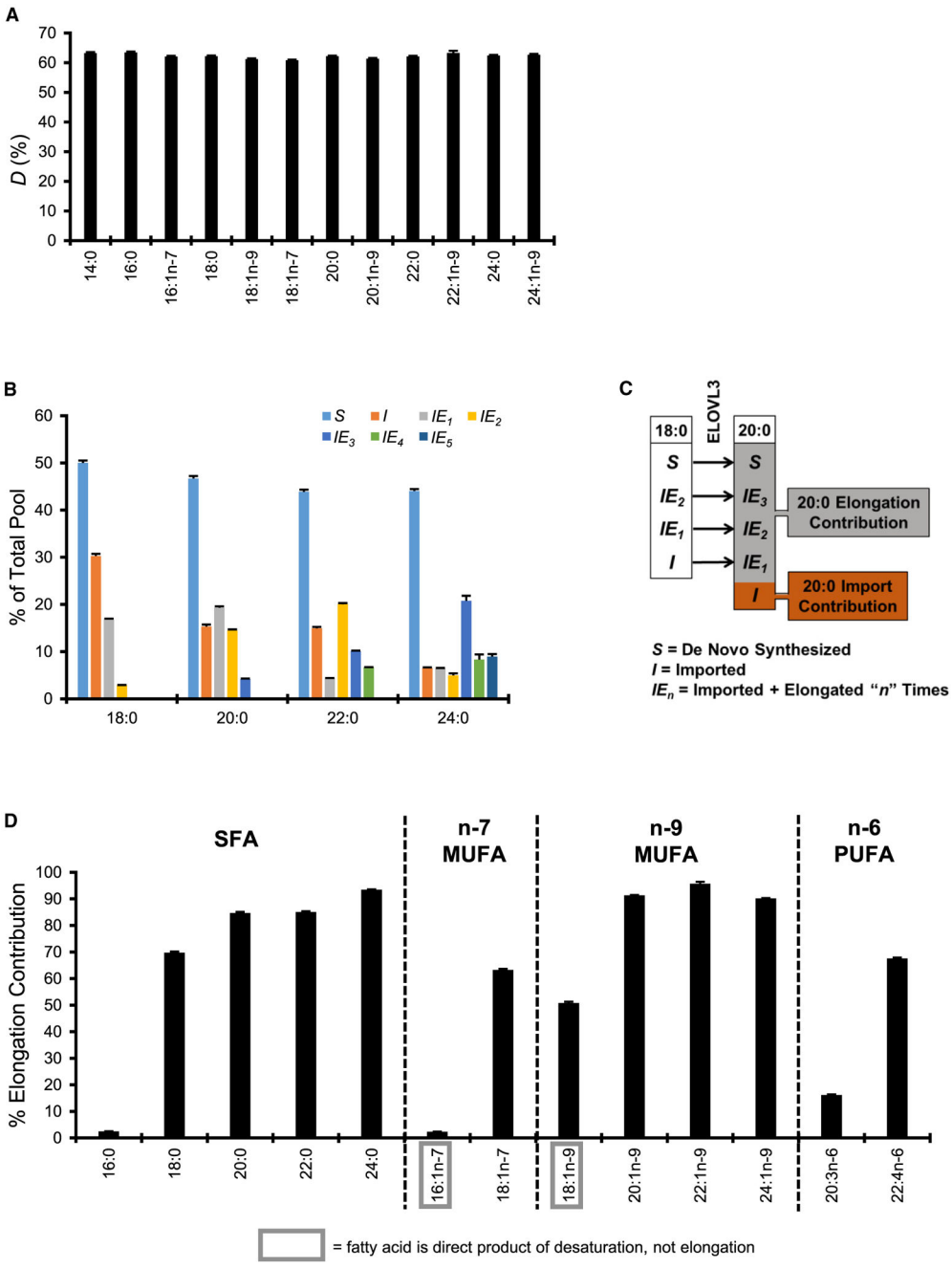

Figure 4. Application of FASA to Cells at iSS and mSS Reveals a Significant Role for Elongation

H1299 cells were cultured in a sub-confluent state for 5 days in medium containing 5% FBS and 100% U-$^{13}C_6$-glucose to achieve iSS and mSS. On day 5, cells were collected, and isotopologue distributions were determined for fatty acids.

(A) FASA-derived *D* parameter values from the indicated SFAs and MUFAs.

(B) FASA-derived contribution parameters for selected SFA pools.

(C) Diagram for determining elongation and import contribution possibilities to the 20:0 pool.

(D) Elongation contribution for the indicated SFAs, MUFAs, and PUFAs. When applying FASA to PUFAs (but not SFAs or MUFAs), values for D_0, D_1, and D_2 were fixed using results from 16:0 to facilitate modeling. Data shown are the average ± SD of biological quadruplicates.

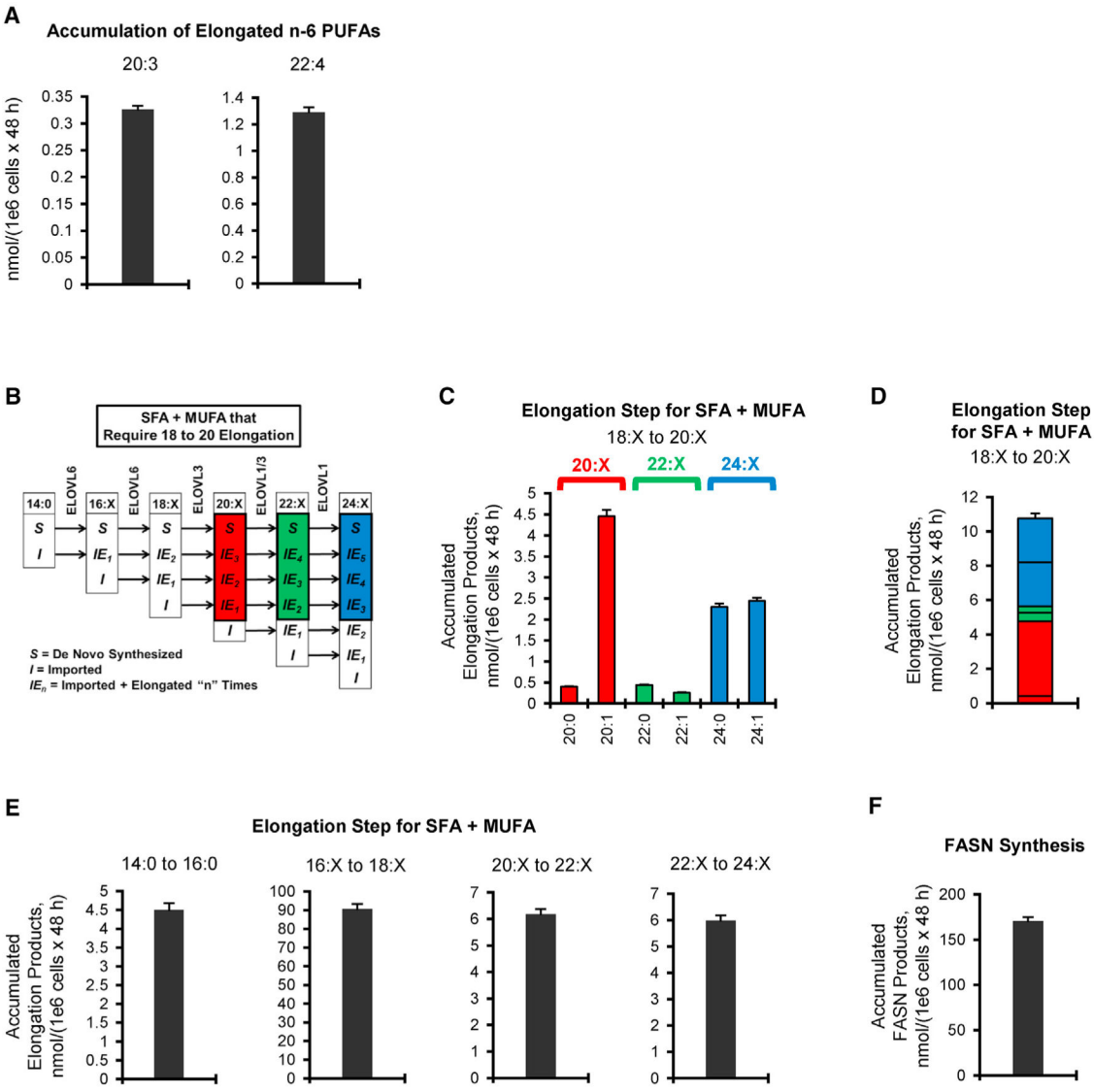

Figure 5. Interpretation of FASA-Derived Parameters from Fatty Acid Pools Not at iSS and/or mSS

H1299 *shCON* cells were treated with 15 ng/mL doxycycline for 96 hr. In the final 48 hr of doxycycline treatment, they were also labeled in medium containing 5% FBS, 100% U-$^{13}C_6$-glucose, and 100% U-$^{13}C_5$-glutamine. After 48 hr of labeling, cells were counted on-plate, collected, and analyzed for fatty acid content. When applying FASA, D_0, D_1, and D_2 values for all fatty acids were fixed using results from 16:0 to facilitate modeling.

(A) Accumulated n-6 PUFA elongation products.

(B) Schematic for which SFA and MUFA origins require 18-to-20 elongation; X = 0 or 1 desaturations in fatty acids.

(C) Accumulated 20-, 22-, and 24-carbon SFAs and MUFAs that were subject to 18-to-20 elongation during the 48-hr labeling period.

(D) Summation of all accumulated 18-to-20 elongation products as described in (C).

(E) Accumulated SFA and MUFA elongation products.

(F) Accumulated FASN products.

For (B)–(D), red, green, and blue indicate contributions from 20-, 22-, and 24-carbon fatty acids, respectively. Values represent average ± SD of biological quadruplicates.

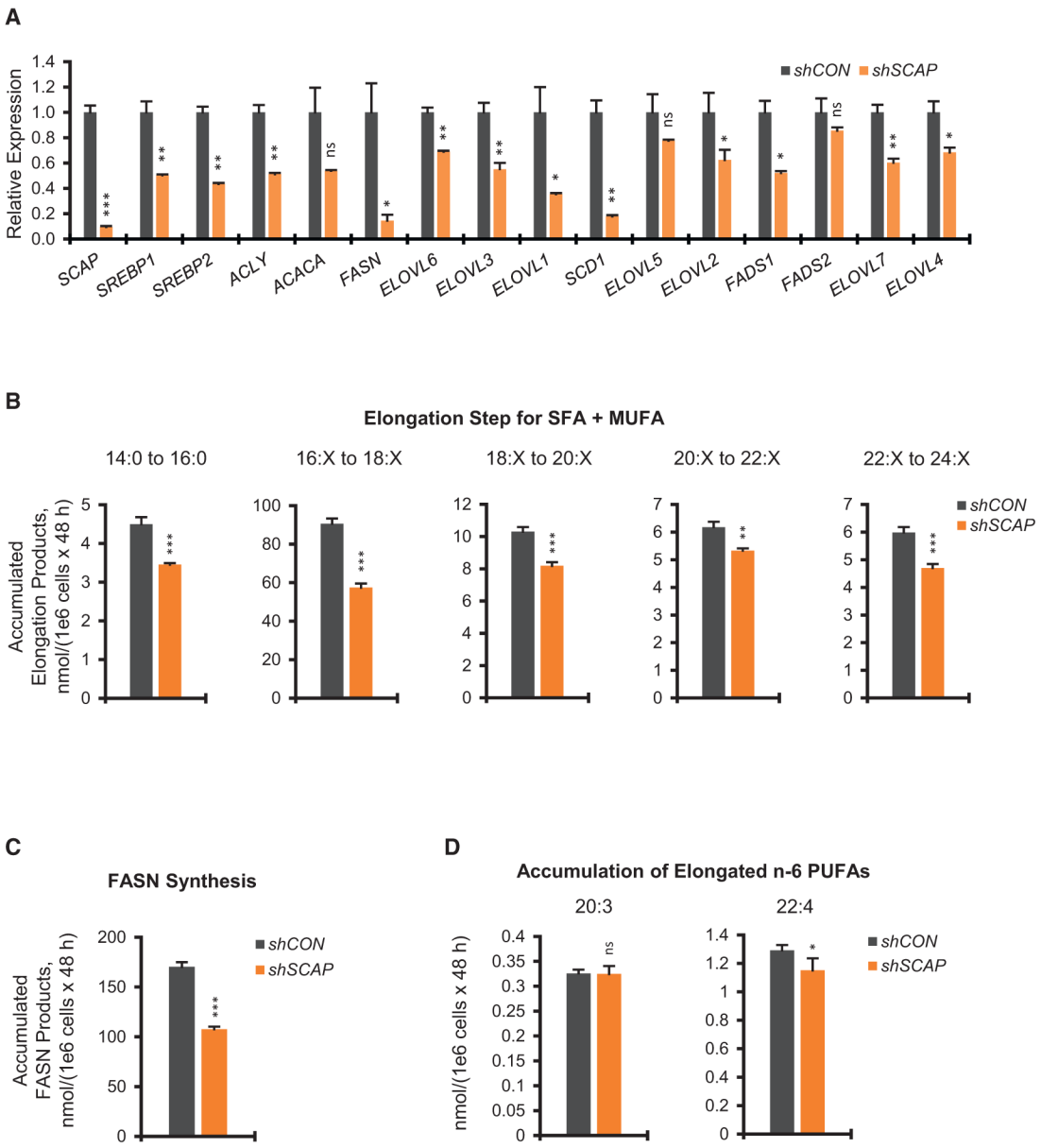

Figure 6. Application of FASA to Cells with Acute Metabolic Change by Silencing of SREBP

H1299 *shCON* and H1299 *shSCAP* cells were treated with 15 ng/mL doxycycline for 96 hr. In the final 48 hr of doxycycline treatment, they were also labeled in medium containing 5% FBS, 100% U-$^{13}C_6$-glucose, and 100% U-$_{13}C_5$-glutamine. After 48 hr of labeling, cells were collected for gene expression analysis or counted on-plate and collected for fatty acid analysis. When applying FASA, D_0, D_1, and D_2 values for all fatty acids were fixed using results from 16:0 to facilitate modeling.

(A) mRNA expression of *SCAP* and selected SREBP targets with doxycycline.

(B) Accumulated SFA and MUFA elongation products.

(C) Accumulated FASN products.

(D) Accumulated n-6 PUFA elongation products.

Values represent average ± SD (n = 3 for RNA, n = 4 for fatty acids). ns (not significant) $p \geq 0.05$, *$p < 0.05$, **$p < 0.01$, and ***$p < 0.001$ (two-tailed heteroscedastic Student's t test).

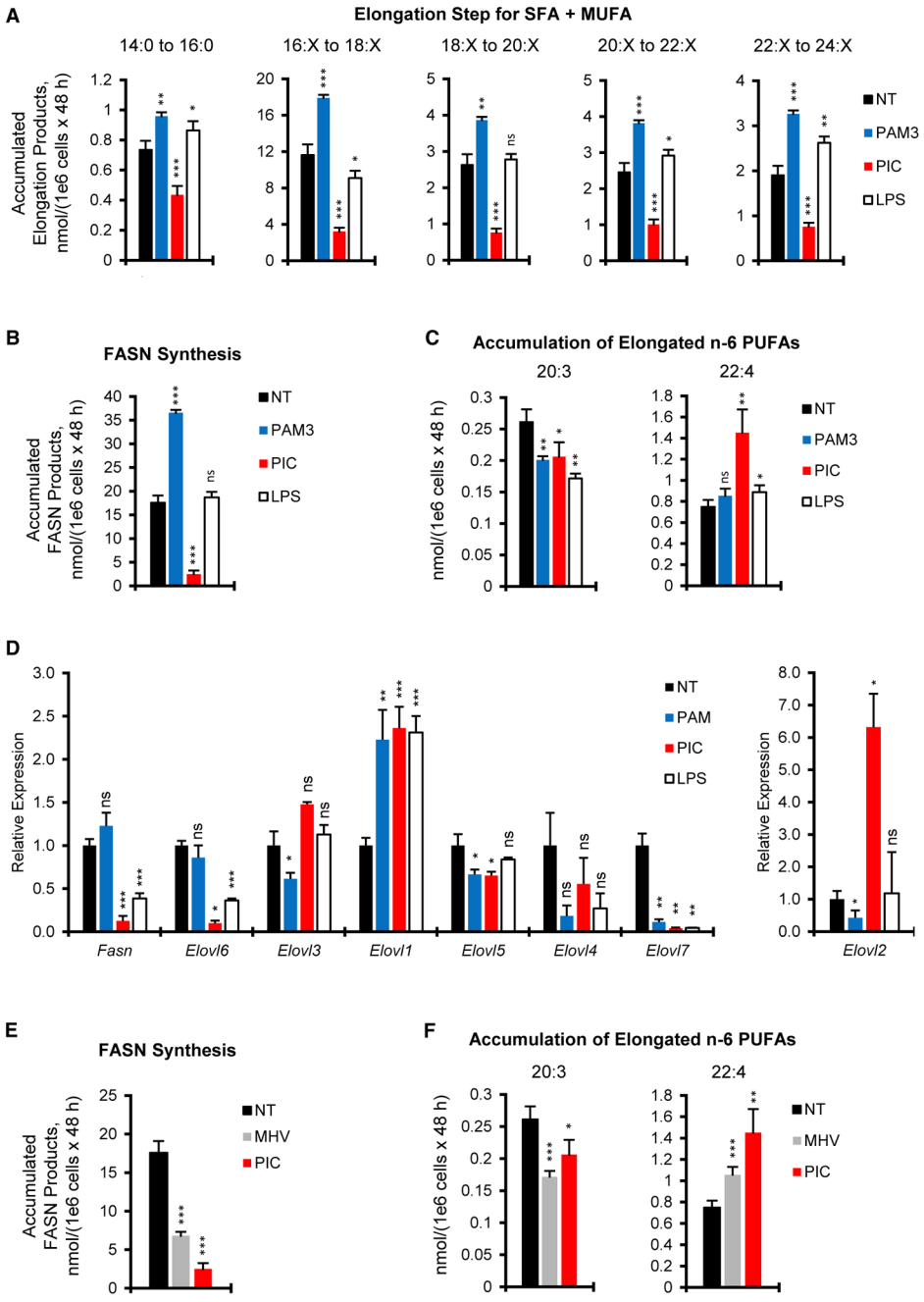

Figure 7. Metabolic Reprogramming of Fatty Acid Elongation Programs by TLRs

BMDMs were treated with a TLR2 agonist (Pam3CSK4 [PAM3], 50 ng/mL), a TLR3 agonist (poly(I:C) [PIC], 1,000 ng/mL), or a TLR4 agonist (LPS, 50 ng/mL) or infected with MHV-68 (MOI = 1) in medium containing 5% FBS, 100% U-$^{13}C_6$-glucose, and 100% U-$^{13}C_5$-glutamine for 48 hr. Cells were collected after 24 h of labeling for gene expression analysis or counted on-plate and collected after 48 hr of labeling for fatty acid analysis. When applying FASA, D_0, D_1, and D_2 values for all fatty acids were fixed using results from 16:0 to facilitate modeling.

(A) Accumulated SFAs and MUFAs that were subject to the indicated elongation step for non-treated (NT) and TLR-activated macrophages.
(B) Accumulated SFAs and MUFAs that were synthesized by FASN for NT and TLR-activated macrophages.
(C) Accumulated n-6 PUFAs that were elongated in NT and TLR-activated macrophages.
(D) mRNA expression of *Fasn* and *Elovl1-7* for NT and TLR-activated macrophages.
(E) Accumulated FASN products for NT, PIC-treated, and MHV-68-infected macrophages.
(F) Accumulated n-6 PUFA elongation products for NT, PIC-treated, and MHV-68-infected macrophages.
Values represent average ± SD of biological quadruplicates. ns (not significant) $p \geq 0.05$, *$p < 0.05$, **$p < 0.01$, and ***$p < 0.001$ (two-tailed heteroscedastic Student's t test). See also Figure S12 and Table S3.

KEY RESOURCES TABLE

REAGENT or RESOURCE	SOURCE	IDENTIFIER
Bacterial and Virus Strains		
MHV-68	Ting-Ting Wu (UCLA)	N/A
Chemicals, Peptides, and Recombinant Proteins		
DMEM	Thermo Fisher	Cat# 11965-118
DMEM (no glucose)	Thermo Fisher	Cat# 11966-025
DMEM (no glucose, no glutamine, no phenol red)	Thermo Fisher	Cat# A14430-01
RPMI 1640	Thermo Fisher	Cat# 11875-119
RPMI 1640 (no glucose)	Thermo Fisher	Cat# 11879-020
Optimem I	Thermo Fisher	Cat# 31985
FBS	Omega Scientific	Cat# FB-11
FBS	Atlanta Biosciences	Cat# S11150
FBS	VWR	Cat# 89510-186
FBS	HyClone	Cat# 16777-014
Penicillin/streptomycin	Thermo Fisher	Cat# 15140122
HEPES	Thermo Fisher	Cat# 15630-080
Sodium pyruvate	Thermo Fisher	Cat# 11360070
MEM non-essential amino acids solution	Thermo Fisher	Cat# 11140-050
L-glutamine	Thermo Fisher	Cat# A2916801
Trypsin-EDTA	Thermo Fisher	Cat# 25200-056
FuGENE 6	Promega	Cat# E2691
Blasticidin	Invivogen	Cat# ant-bl-1
Puromycin	Gemini	Cat# 400128P100MG
RBC lysis buffer	Sigma-Aldrich	Cat# R7757
Recombinant M-CSF generated from CMG14-12 culture supernatant	Takeshita et al., 2000	N/A
Dharmafect 4	Thermo Fisher	Cat# T-2004-03
U-$^{13}C_6$-D-glucose (MPT grade)	Cambridge Isotopes Laboratories	Cat# CLM-1396-MPT-PK
U-$^{13}C_5$-L-glutamine (MPT grade)	Cambridge Isotopes Laboratories	Cat# CLM-1822-H-MPT-PK
Doxycycline hyclate	Sigma-Aldrich	Cat# D9891-10G
Pam3CSK4	Invivogen	Cat# tlrl-pms
Poly(I:C)	Invivogen	Cat# tlrl-pic
Lipopolysaccharaide (LPS)	Invivogen	Cat# tlrl-smlps
Trypan blue stain solution	Thermo Fisher	Cat# ICN1691049
Acridine Orange	Thermo Fisher	Cat# A1301
Propidium Iodide	VWR	Cat# 80057
Calcein AM	Santa Cruz Biotechnologies	Cat# sc-203865
TRIzol	Thermo Fisher	Cat# 15596026
GLC-96 (methyl esters)	Nu-Chek Prep	Cat# GLC-96
18:1n-7 methyl ester	Nu-Chek Prep	Cat# U-48-M
19:0 methyl ester	Nu-Chek Prep	Cat# N-19-M

REAGENT or RESOURCE	SOURCE	IDENTIFIER
Critical Commercial Assays		
High-Capacity cDNA Reverse Transcription Kit	Applied Biosystems	Cat# 4368813
KAPA SYBR FAST qPCR Master Mix (2X) optimized for LightCycler 480	KAPA Biosystems	Cat# KK4601
Gateway LR Clonase II	Thermo Fisher	Cat# 11791-020
Experimental Models: Cell Lines		
NCI-H1299	ATCC	Cat# CRL-5803; RRID:CVCL_0060
H1299 *shCON*	This paper	N/A
H1299 *shSCAP*	This paper	N/A
Murine bone marrow-derived macrophages	Generated at UCLA	N/A
Primary Human Fibroblasts	Coriell Institute	Cat # ND38530; RRID:CVCL_EZ28
293FT	Harvey Herschman (UCLA)	N/A
Experimental Models: Organisms/Strains		
Mouse: C57BL/6J	The Jackson Laboratory	RRID: IMSR_JAX:000664
Oligonucleotides		
siControl	GE Dharmacon	Cat# D-001810-02-05
siELOVL1	GE Dharmacon	Cat# L-009355-01-0005
See Table S4 for shRNA sequences	This paper	N/A
See Table S4 for qPCR primer sequences	This paper	N/A
Recombinant DNA		
pENTR/H1/TO	Thermo Fisher	Cat# K4920-00
pLentipuro/BLOCK-iT-DEST	Abel et al., 2013	N/A
pLP1	Thermo Fisher	Cat# K4975-00
pLP2	Thermo Fisher	Cat# K4975-00
pLP/VSV-G	Thermo Fisher	Cat# K4975-00
pLenti0.3/EF/GW/IVS-Kozak-TetR-P2A-Bsd	Abel et al., 2013	N/A
Software and Algorithms		
Natural Isotope Abundance Correction Algorithm	This paper	N/A
convISA	Tredwell and Keun, 2015	N/A
Fatty Acid Source Analysis (FASA)	This paper	https://github.com/BensingerLab/FASA